INSTITUTO SUPERIOR DE ENGENHARIA DO PORTO
MESTRADO EM ENGENHARIA ELECTROTÉCNICA E DE COMPUTADORES



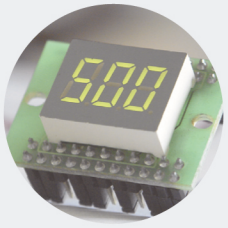


BatEval Study on different battery technologies for IoT

AFONSO SERRA DUQUE
Setembro de 2023

POLITÉCNICO
DO PORTO

Politécnico do Porto
Instituto Superior de Engenharia do Porto

BatEval – Study on different battery technologies for IoT

Afonso Serra Duque

Master in Electrical and Computer Engineering
Specialization Area of Automation and Systems

Departamento de Engenharia Eletrotécnica
Instituto Superior de Engenharia do Porto

September, 2023

This dissertation partially satisfies the requirements of the Thesis/Dissertation course of the program Master in Electrical and Computer Engineering, Specialization Area of Automation and Systems.

Candidate: Afonso Serra Duque, No. 1180951, 1180951@isep.ipp.pt

Scientific Guidance: Paula Maria Marques Moura Gomes Viana, pmv@isep.ipp.pt

Co-advisor: José Meira, jose.meira@fraunhofer.pt

Company: Fraunhofer Portugal AICOS

Advisor: Diogo Correia, diogo.correia@fraunhofer.pt

Departamento de Engenharia Eletrotécnica
Instituto Superior de Engenharia do Porto
Rua Dr. António Bernardino de Almeida, 431, 4200–072 Porto

September, 2023

Acknowledgements

First of all, I would like to thank Fraunhofer Portugal AICOS (FhP) for allowing me to do my internship in their working environment and with a great team. Not only that, but I'd also like to thank Instituto Superior de Engenharia do Porto (ISEP) for the five years of knowledge I've acquired and for being the bridge between students and companies.

Next, I would like to thank my supervisors Paula Viana (ISEP) and Diogo Correia (FhP) for the various suggestions and knowledge they showed me. To my co-supervisor José Meira (FhP) for helping me collect data using the measuring devices at my disposal. I would also like to thank Tomás Pereira (FhP) for helping me select the machine learning algorithm that was best suited to my project.

I would also like to thank my friends and colleagues at ISEP for making these five years memorable.

Finally, I would like to thank my parents and my girlfriend for accompanying me throughout these 5 years, giving me the support I needed to overcome all the obstacles that came my way.

Abstract

Nowadays, all electronic devices need a power supply to function as intended. This source can be the power grid, which runs through the domestic or urban electricity supply, or a portable power supply for devices that can be used on a day-to-day basis in any location. From the latter, batteries have emerged that are used in devices such as smartphones or power tools. These are capable of storing energy in a reduced format, thus increasing the mobility of these devices.

In this work we provide an analysis of two types of batteries: those that are available for sale on the market, and those that are still being developed by laboratories or companies. These batteries differ one from the other, especially in terms of their chemistry and size, as well as other electrical parameters such as voltage and capacity.

After analysing the existing chemistries on the market, an algorithm was developed to select the battery that best suits the specifications of the project the user is working on. This algorithm takes into account parameters such as an operating temperature range (minimum and maximum limit), as well as the desired capacity and mass of the desired battery.

Keywords:Battery analysis, IoT, kNN, Remote Data Acquisition, RTD

Resumo

Atualmente, todos os dispositivos eletrónicos necessitam de uma fonte de alimentação para funcionarem como pretendido. Esta fonte pode ser a rede energética, que passa pela canalização elétrica doméstica ou urbana, ou então uma fonte de alimentação portátil para dispositivos que possam ser utilizados no dia-a-dia em qualquer localização. Destas últimas, surgiram as baterias que são utilizadas em dispositivos como smartphones ou ferramentas elétricas. Estas são capazes de armazenar energia num formato reduzido, aumentando assim a mobilidade destes dispositivos.

Este trabalho faz uma análise de dois tipos de baterias: as que estão disponíveis para venda no mercado, e as que ainda estão a ser desenvolvidas por laboratórios ou empresas. Estas baterias diferem entre sí especialmente no que toca à sua química e à sua dimensão, assim como noutros parâmetros elétricos tal como a tensão e a capacidade.

Após esta análise das químicas exitentes no mercado, foi desenvolvido um algoritmo que permite, de entre um conjunto definido, selectionar a bateria que mais se adequa às especificações do projeto que o utilizador está a trabalhar no momento. Este algoritmo considera parâmetros como um intervalo de temperatura de operação (limite mínimo e máximo), assim como a capacidade pretendida e a massa da bateria pretendida

Palavras-Chave: Análise de baterias, IoT, kNN, Aquisição Remota de Dados, RTD

Contents

List of Figures

List of Acronyms

CALCE	Center for Advanced Life Cycle Engineering
CC	Constant Current
CV	Constant Voltage
DST	Dynamic Stress Test
ECG	Electrocardiogram
EIS	Electrochemical Impedance Spectroscopy
IoT	Internet of Things
KNN	K-Nearest Neighbours
KOH	Potassium Hydroxide
Li-ion	Lithium-ion
LiPo	Lithium Polymer
ML	Machine Learning
Na-ion	Soium-ion
NaS	Sodium-Sulfur
NASA	North American Space Agency
Ni-Cd	Nickel-Cadmium
NiMH	Nickel-Metal Hydrate
NiOOH	Nickel Oxohydroxide
NTC	Negative Temperature Coefficient
OCV	Open-Circuit Voltage
PCoE	Prognostics Center of Excellence
PSO	Particle Swarm Optimization

RMSE	Root Mean Square Error
RTD	Resistance Temperature Detector
SCPI	Standard Commands for Programmable Instruments
SoC	State of Charge
SoH	State of Health
SRM	Structural Risk Minimization
SVM	Support Vector Machine
UDDS	Urban Dynamometer Driving Schedule
UKF	Unscented Kalman Filter
VISA	Virtual Instrument Software Architecture

Chapter 1

Introduction

This chapter provides an overview to the topic of the thesis, introducing requirements and challenges related to the need of selecting the appropriate battery for standalone devices. Additionally, this chapter also defines the objectives behind the development of the project.

1.1 Contextualization

In our daily lives, we interact with several electronic devices. From simple devices such as lamps or chargers to more complex ones such as phones and televisions, all require a power source to work as intended.

For devices suited for fixed locations (televisions, lamps, or appliances), the usual source of power is the electrical grid supplier, whose electrical current is accessible through electrical outlets. These devices are not required to be movable due to their size and function specifications. However, for several scenarios that include mobility or outdoor usage, this solution is not adequate. In the case of apparatus such as smartphones, smartwatches and power tools, they do not need to remain fixed when used. Due to their variety of uses, portable devices require an external power supply capable of conveying energy throughout the time the machine is working.

This demand for portable energy resulted in the appearance of portable batteries, containers of chemicals whose reactions resulted in the generation of electrons. The emergence of these devices allowed for the portability of electronic circuits without the demand of being limited to the length of the powering cable connected to the

energy grid, as well as the experimentation of different reagents in order to improve battery performance and diminish its size.

However, with the diversity of battery chemistries, dimensions and other intrinsic characteristics (operating temperature, number of charging cycles and overall performance), these mobile devices began to have a large set of batteries to choose from. At the moment, the ones that are commonly used (and usually are the default choice of most manufacturers) are batteries whose chemistries are based on lithium [1]. Moreover, the selection of these chemistries is not always the most correct, mainly due to the environmental impact of the reagents in the eventuality of a leak [2]. For this reason, an approach to assist hardware designers in ranking chemistries to be used in a given scenario would have a positive impact. Given this, this thesis proposes an algorithm that helps in this decision making process.

1.2 Goals

The main goal of this dissertation is to make a review of the different batteries that are available on the market, in addition to others that are emerging but are not ready yet for public use. The different solutions should be analyzed in terms of their performance, reagents used, functioning principles and temperatures of operation.

In a next step, an algorithm for assisting hardware designers should be developed. This algorithm should consider several parameters characteristic of battery study:

- Voltage
- Capacity
- Temperature of Operation
- Sustainability

In order to be able to test and validate the proposed decision making algorithm, a set of batteries should be submitted to different functioning scenarios and data collected.

1.3 Dissertation Structure

The document is organized as follows:

- Chapter 1: Introduction of the problem and project's goals.
- Chapter 2: Review of traditional and emerging battery technologies. Identification and description of different battery analysis methods. Review of battery datasets, and the processes used for their creation.

- Chapter 3: Description of the project, from the hardware and software specifications to the setup of the devices used. Analysis of the results obtained.
- Chapter 4: Conclusions from the project and future work to be implemented.

Chapter 2

State of the Art

This chapter provides a theoretical analysis of the project that is going to be developed. This analysis starts with the description of several battery chemistries, both traditional and solutions under development (sub-chapter 2.1), followed by the presentation of different mechanisms used for the acquisition of data (sub-chapter 2.2) as well as algorithms that are often used in classification or regression problems (sub-chapter 2.3). Finally, at the end of this chapter, there are going to be presented several datasets created by authors and corporations that can be used for a range of applications based on the techniques given at sub-chapters 2.2 and 2.3 (sub-chapter 2.4)

2.1 Battery chemistries

Nowadays, there are two types of batteries on the market: primary and secondary. Primary batteries, also known as non-rechargeable batteries, cannot be charged when their working capacity is close to zero. This is the case of Alkaline cells and Zinc-air cells.

However, these types of batteries quickly began to be overpast by secondary batteries, whose internal structure is represented in figure 2.1. This is given to the fact that secondary, or rechargeable, batteries are meant to be discharged and charged many times, resulting in a reduction of hazardous waste [3]. Not only that, but rechargeable batteries are also cheaper to produce ($7.85/kWh vs $166/kWh of non-rechargeable batteries)[4].

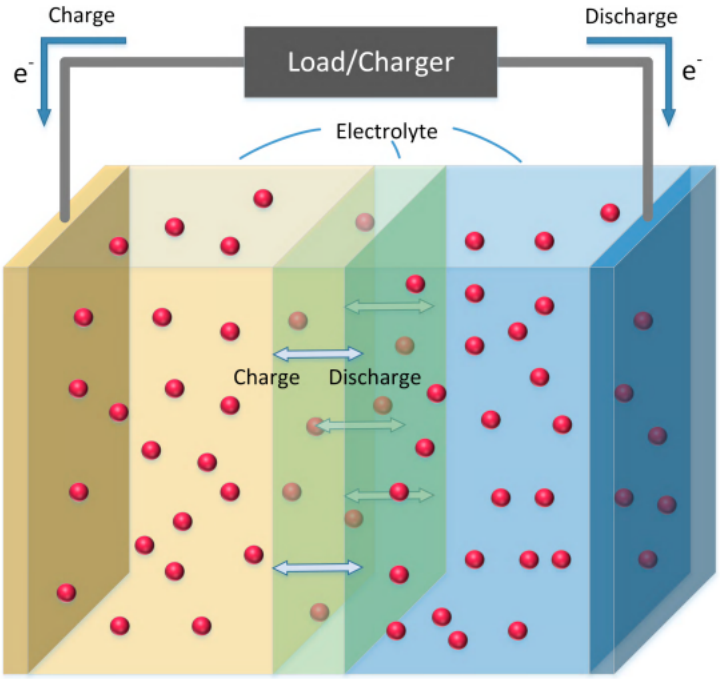

Figure 2.1: Internal structure of a battery [5]

Every type of battery has in its electrical constitution two poles, one positive (named anode) and one negative (named cathode), separated by a thin membrane, called a separator, to prevent the battery from short-circuiting. A substance, called an electrolyte, embeds those components to facilitate ion transference inside the battery. This electrolyte can be present in two states, solid (characteristic of dry battery cells) or liquid (characteristic of wet battery cells). The alteration of the physical state of the electrolyte often results in the alteration of some usability cares. While liquid electrolytes offer a higher ionic conductivity, they pose concerns regarding their leakage and flammability. In the use of solid electrolytes, at the cost of reducing ionic conductivity, these substances reduce the event of leakages and internal crystallization [6].

Inside the battery, on a chemical level, there are two types of reactions responsible for the generation of electrons and ions from atoms (oxidation, happening on the anode) and the generation of atoms from electrons and ions (reduction, happening on the cathode). From these two products, while ions move from the anode to the cathode through the separator, electrons do not use the same path. The separator allows the passage of ions but is a barrier for electron movement. Due to this barrier, electrons' trajectory has the same direction (from the anode to the cathode), but instead of moving inside the battery, they flow through an external circuit. If the electrons were to flow internally between poles, it would cause a short circuit rendering the battery unusable.

These batteries have a number of characteristics that can give you an advantage in different circumstances. These characteristics are [7]:

- **Nominal Voltage**

  Voltage that is measured between the positive and negative poles of a cell, and it is measured in Volt (V). It represents the pressure that a battery makes in pushing electrical current to the external circuit. In most cases, several batteries are used in series or in parallel, whether to provide a more durable voltage or current source. This information is given by the manufacturer, being commonly inscribed on the battery itself.

- **State of Charge (SoC)**

  This parameter is defined as being the quotient between the capacity of the cell in a given instant, and the nominal capacity of the cell. This value is expressed in percentage and can have a value that ranges from 0% to 100%, which means that the cell is either completely discharged or fully charged, respectively[8].

- **Self-Discharge Rate**

  A battery does not have the same characteristics over time. Because air allows electricity to circulate around, the battery is continuously connected to some sort of man-made or natural circuit. The concept behind this is called Self-Discharge rate, and it is responsible for the slow drain of a battery. This is visible whenever a cell is left fully charged and unused. After some time, when the battery is about to be used, it has a lower capacity than it had when it was fully charged. This characteristic can be calculated through equation 2.1, where SoC represents the State of Charge in a given instant. (SoC_1 and SoC_2 represent the State of Charge of the battery in two different instants)

$$\text{Self-Discharge Rate} = \frac{SoC_1 - SoC_2}{SoC_1} \tag{2.1}$$

  This value is related to the electrical conductivity of the environment where the battery is set in. In the example where there isn't anything involving the battery (thus being involved in air), the electrical conductivity, which is the inverse of electrical resistance, has a low value of approximately 10^{-12} S/m [9], meaning that the air offers a high resistance for conducting electricity and thus contributing to a low self-discharge rate.

- **Energy Capacity**

  The capacity of a battery corresponds to the amount of energy that it can store and release. Despite the SI unit for energy being Joule (J), which simplifies

the comparison between reactions (those being chemical, mechanical or nuclear), manufacturers opt to use the Ampère-hour (Ah) and its submultiples. Capacity is calculated using equation 2.2.

$$\text{Capacity (Ah)} = \text{Current supplied (A)} \times \text{Discharge Duration (h)} \tag{2.2}$$

- **Specific Energy**

  Specific energy is defined as the amount of energy that can be stored in a battery per unit of mass. The reason why this parameter is of significant importance is because its value differs depending on the reagents used for the internal reaction. As a consequence, this selection of chemicals can result in a better energy source with a small size format. It can be calculated according to the equation 2.3, with table 2.1 depicting values of specific energy for most commonly used batteries.

$$\text{Specific Energy (Wh/kg)} = \frac{\text{Nominal Voltage (V)} \times \text{Capacity (Ah)}}{\text{Battery Mass (kg)}} \tag{2.3}$$

Type of Battery	**Specific Energy (Wh/kg)**
Lead-Acid[10]	25-35
Nickel-Cadmium (Ni-Cd)[11]	50-75
Nickel-Metal Hydrate (NiMH)[12]	50-110
Lithium-ion/Lithium Polymer (Li-ion/LiPo)[13]	250-670

Table 2.1: Specific Energy of different batteries

2.1.1 Commercial solutions

Lead Acid

Lead-acid batteries are usually manufactured with a grid of lead on the cathode and grains of lead oxide on the anode, while being submerged in an electrolyte made of a strong acid (usually sulfuric acid). These batteries have 12 V, a low cycle durability, an energy efficiency ranging from 80 to 90% and a self-discharge rate of 10-15% [14]. These batteries are commonly used in the automotive industry and in the production of emergency power supplies [10].

Regarding the construction of the battery, specifically the area regarding the cathode, there are two different types of lead plates used:

- Pasted flat plates - Due to their simplicity in design, these plates are easy to mass produce by casting. These components are manufactured mainly through

the process of metal casting[15]. These grids are made like the one in figure 2.2a.

- Tubular plates - This plate, represented in figure 2.2b, consists on a series of tubes, welded to a common bus, that contain a metal spine and the material present in the anode, lead oxide. This type of assembly reduces the chemical's leak due to the tubes being set side by side[15].

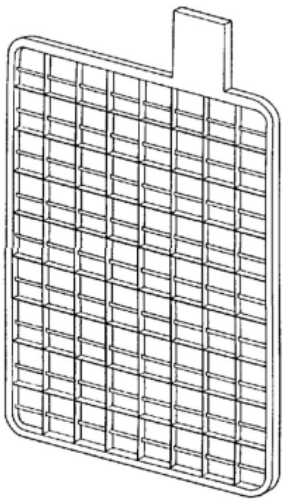

(a) Flat plate[15]

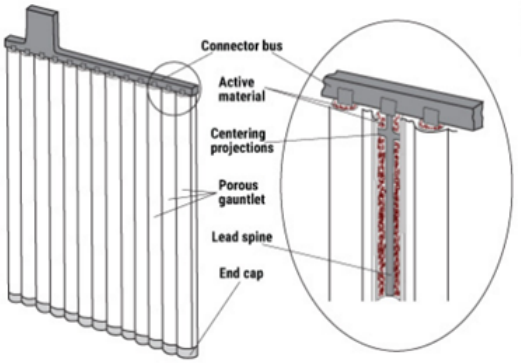

(b) Tubular plate[15]

Despite being a simple and cheap power supply (costing between $100 and $200 per kWh [16]), it is also a battery that has a harmful effect on the environment. The main two components of this battery, lead and sulfuric acid, are products harmful to the soil as well as to the human being. Sulfuric acid can poison water and soil, which results in the death of plants and poisoning of the land. Additionally, lead is a heavy metal which, in high quantities, can pose a severe health risk to the human heart and kidney[17][18]. Table 2.2 summarizes this section, referencing all of the more important characteristics of this technology.

Chemistry	Lead-Acid
Nominal Voltage	12V
Self-Discharge Rate	10-15%
Use cases	- Emergency Power Supplies - Automotive industry
Production Cost per kWh	$100 - $200
Disadvantages	- Uses toxic materials (lead and sulfuric acid) - Low energy efficiency (80-90%), as a consequence of low energy density

Table 2.2: Lead-acid Battery Characteristics

Nickel-Cadmium (Ni-Cd)

These batteries are made of nickel oxides in the anode and a mix of cadmium oxide and cadmium metal in the cathode, while submerged in a liquid electrolyte based on Potassium Hydroxide (KOH). They are a better alternative to lead-acid batteries in terms of working temperature (from -65ºC to 60ºC)[19], but they have a higher cost per kWh (between $300 and $600 per kWh).

These batteries have a nominal voltage of 1.2V, a self-discharge rate of 10% and an elevated number of charging cycles [20]. When compared to Lead-acid batteries, Ni-Cd technology has reduced weight and volume. When adding this to the fact that it is capable of storing more energy than its predecessor, this cell started to be used for solar lights and, on an industrial scale, in the avionics sector [21][19].

However, one of the consequences of using these types of cells is a phenomenon known as the "memory effect". It is a consequence of charging a cell to its full capacity in intermittent intervals of time (charging 25%-50% then remove the charger, then charging between 40%-60%). This inconsistent charge of the battery results in the "memorization" of the life cycle, so that instead of charging to full capacity, it is charged up to the "memorized" value[22].

From an environmental perspective, this battery is not the most eco-friendly available on the market. During the manufacturing process, this cell uses primarily heavy, toxic materials (nickel and cadmium), and their disposal has to be made through specific procedures. For this motive, more and more countries are starting to ban the usage of this technology and use more eco-friendly alternatives, such as NiMH, technology which will be explained in the following topic[23]. To sum up this topic, table 2.3 displays the most important information regarding this battery.

Chemistry	Nickel-Cadmium
Nominal Voltage	1.2V
Self-Discharge Rate	10%
Use cases	- Solar Lights - Avionics
Temperature Interval	-65ºC - 60ºC
Production cost per kWh	$300 - $600
Disadvantages	- Uses toxic materials (nickel and cadmium) - Presence of memory effect, thus reducing battery capacity

Table 2.3: Nickel-Cadmium Battery Characteristics

Nickel-Metal Hydrate (NiMH)

These batteries appeared as a replacement for Nickel-Cadmium batteries due to their toxic materials. Its cathode is Nickel Oxohydroxide (NiOOH), similar to its

predecessor, and an anode containing a hydrogen alloy for an anode. These electrodes are wrapped by a liquid electrolyte, usually made of Potassium Hydroxide (KOH). Being NiMH and Ni-Cd batteries similar in terms of their chemistry, their cost of production per kWh is also in the same range ($300 to $600 [16]).

When it comes to its operation characteristics, NiMH cells have a small shelf life of 2 to 5 years with a self-discharge rate of 30% of its capacity and a nominal voltage of 1.2V, with an operating temperature ranging from – 30 to 70ºC, being the optimal interval between 20 and 45ºC [20]. These specifications translate to being a battery that, alongside a reduced environmental impact and a specific energy higher than its predecessor, outclasses Ni-Cd cells in several situations, and it is being used in portable tools, electric vehicles, and small-sized electronics[24].

However, they are still below Li-ion batteries when it comes to energy storage itself. The key discriminators between these two technologies are the specific energy and the cell's self-discharge rate. In these two parameters, li-ion cells have higher specific energy and a low self-discharge rate, affecting the amount of energy that can be stored and maintained for long periods of time[25]. The most important information regarding this battery is present in table 2.4.

Chemistry	Nickel-Metal Hydrate
Nominal Voltage	1.2V
Self-Discharge Rate	30%
Use Cases	- Automotive vehicles - Small Electronics
Temperature Interval	20ºC - 45ºC. Maximum interval is -30ºC - 70ºC
production Cost per kWh	$300 - $600
Disadvantages	- High self-discharge rate, resulting in a smaller shelf life

Table 2.4: Nickel-Metal Hydrate Battery Characteristics

Lithium-ion (Li-ion or LIB)

Lithium-ion batteries are dry cells constructed with an anode made of carbon and a cathode made of a substance containing lithium oxide, usually lithium cobalt oxide, lithium nickel oxide or lithium copper oxide. Its electrolyte consists of lithium salts, such as lithium hexafluorophosphate (LiPF6), dissolved in an organic solvent such as ethylene carbonate. This medium of ionic conductivity is usually present in a liquid state, facilitating the transport of ions through the separator membrane to the anode as well as electrons through an external circuit to the anode[26][27].

Regarding its electrical characteristics, it has a nominal voltage of 3.6 V (which is an assembly of 3 1.2V cells in series) and it can have different sizes from coin-sized to having the same appearance as a lead-acid battery. It also has a high charging cycle

(between 1000 and 10000) and a low self-discharge rate (between 5 and 10%)[20]. So, due to its high capability to provide power in a small size factor, as well as being capable of holding its state of charge for long periods of time, made this cell the default go-to when selecting batteries for powering electronic circuits[23].

Its operating temperature has an ideal interval that ranges between 15 and 35ºC. Prolonged exposure of these types of batteries to temperatures higher than 45ºC results in the reduction of its longevity and consequential degradation and quicker discharge of the battery, while exposure to temperatures lower than 15ºC decreases the rate at which the chemical reactions happen, resulting in lower current that the battery can supply[23]. This failure of chemical reactions can cause the crystallization of lithium on the anode, thus reducing the capacity of the cell. The temperature variation of these batteries can be analyzed in figure 2.3.

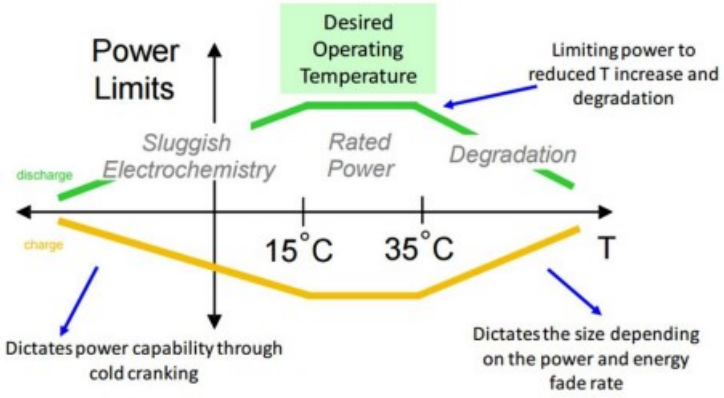

Figure 2.3: Effects of temperature on a Li-ion cell[23]

However, this technology is far from being optimal for all situations. Manufacturers try to minimize any sort of upcoming problem by giving the specifications of the battery pack they developed, such as working temperatures, current values to be expected from charging and discharging, dimensions of the physical pack and its capacity, as well as manufacturing a protection module, represented in figure 2.4, responsible for prevention of processes that may harm the battery internally such as overcharging/overdischarging, short circuit and overheating.

Moreover, this type of cell has a significant impact on the planet. The extraction of lithium can occur on either mining deposits, which can be removed with traditional mining equipment, or on salt deserts. This second alternative, despite being cost-efficient, removes water from locations surrounding the desert and, in those same locations, injects chemicals below the surface, which can contaminate the soil, air and water supplies[26]. Another component that is mainly used in this technology is cobalt, although companies such as CATL and Tesla started making batteries that do not use cobalt [29]. This metal's high demand is a result of the increase in battery manufacturing. It is mined primarily in the Dominican Republic of Congo, but it can

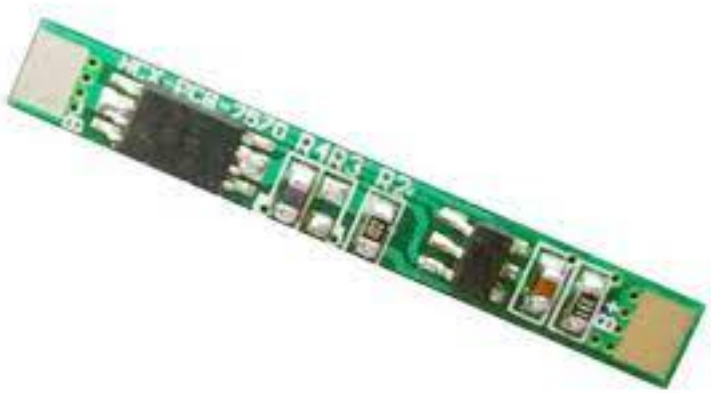

Figure 2.4: Protection circuit module for li-ion batteries[28]

be found in other countries such as Russia and Australia, usually in copper or nickel deposits [26]. However, in the areas where these deposits are located, focusing on the largest miner of cobalt i.e. the Republic of Congo, there are traces of high levels of radioactivity from local deposits of uranium that can pollute nearby rivers and water sources [30]. Furthermore, another problem of cobalt mining resides in human rights violations such as low mining safety and the use of child labor. According to the United States Department of Labor, at least 25000 children work in cobalt mines in the Republic of Congo[31].

Despite these specifications, the battery can still be subjected to performance degradation and, in consequence, cause hazards ranging from swelling to exploding and causing fire and release of toxic fumes[2]. This is what happened in 2016, when smartphone company Samsung recalled all Galaxy Note 7 models, which had reports of spontaneously catching fire and sometimes explode[32]. Table 2.5 summarizes the information of this section.

Chemistry	Lithium-ion
Nominal Voltage	3.6V
Self-Discharge Rate	5-10%
Temperature Interval	15ºC - 35ºC
Production Cost per kWh	$100
Disadvantages	- Lithium extraction can result in sterile or dry soils - More subject to performance degradation

Table 2.5: Lithium-ion Battery Characteristics

2.1.2 In-development solutions

The previous battery technologies are widely used and are widely available on the market. However, the development of new batteries comes in handy for replacement

of the previous ones, for problems regarding the cost of manufacturing and purchasing, its environmental impact and dimensions of the battery itself. In this topic, it is going to be presented several batteries that are under development, either with new materials or adapting new batteries with other compounds.

Sodium-Sulfur (NaS)

These batteries, as the name implies, have on the negative and positive electrodes molten sodium and molten sulfur. However, unlike other types of batteries, which use liquid or gel-like electrolytes, NaS batteries use a solid ceramic electrolyte. This alteration of the physical state of the electrolyte results in a reduction of battery weight, as a result of the removal of the membrane and casing required to separate the liquid electrolyte in each cell, and a longer battery lifetime, caused by a better isolation of heat resulted from the chemical reactions[33]. Its constitution is visible on figure 2.5.

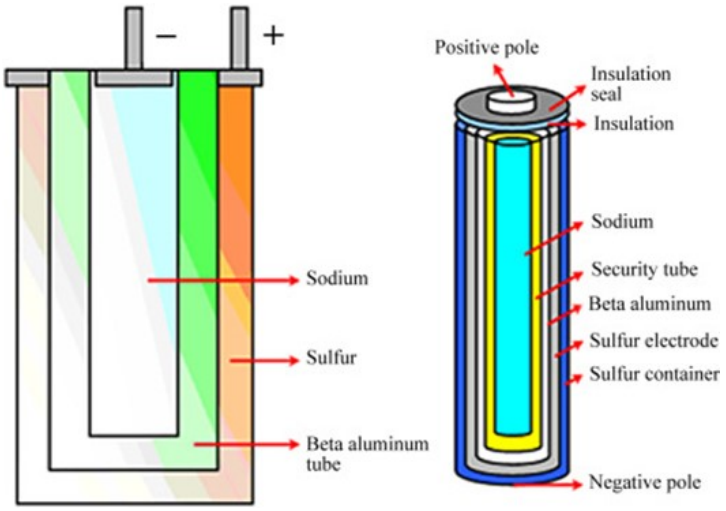

Figure 2.5: Internal characterization of a Sodium-Sulfur cell

It has specific energy ranging from 150 to 240 Wh/kg, with a working voltage of 2 V, a very low self-discharge rate and an average energetic efficiency of about 85%. They are made from recyclable, non-toxic materials that are abundant on the surface of the planet (sodium is indirectly obtained by electrolysis of halite or other sodium-based compounds, while sulfur is obtained naturally on surface deposits)[10].

These batteries have a high working temperature in order to maintain the sodium and sulfur in their molten state, ranging from 574K (300ºC) to 624K (350ºC). Since the extraction of these materials from the processes referred previously is very expensive, NaS cells are made on a large size in order to be more economical to the final user ($300 - $500 per kWh [34]). Due to this temperature interval, this battery is not prepared for small-scale mobile devices. This is given by the fact that the

internal compounds must remain in a molten state, and external heating of the battery is necessary in order to maintain the reagents in that state [35]. Instead, they are recommended for use in stationary high-scale, high-power machines due to an inconvenience caused by a subproduct of the chemical reaction. This subproduct, obtained during the discharge process when sodium ions move from the anode to the cathode and react with the sulfur, which reacts with the electrons traveling from the external circuit, making sodium polysulfide, a highly corrosive material[23]. Table 2.6 summarizes this section of the report.

Chemistry	Sodium-Sulfur
Nominal Voltage	2V
Self-Discharge Rate	$\sim 0\%$[1]
Temperature Interval	300ºC - 350ºC
Production Cost per kWh	\$300 - \$500
Disadvantages	- Generation of harmful compounds (Sodium polysulfide) - High operation temperature and economical factors limits the use of this chemistry for high power machinery

Table 2.6: Sodium-Sulfur Battery Characteristics

Sodium-ion (Na-ion or NIB)

This battery is a variant of the lithium-ion cells. Like li-ion technology, its liquid electrolyte is made of sodium crystals dissolved in an organic compound. The difference between the two resides in their main component. In other words, while lithium is being used for longer, sodium is more abundant and easier to obtain. Sodium is available on all of Earth's crust, as visible in figure 2.6 and is an alkaline metal more reactive than lithium, resulting in higher releases of energy when being used as a reagent on a chemical reaction[36].

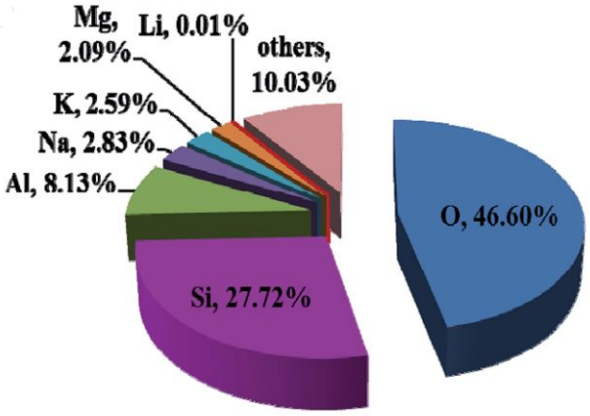

Figure 2.6: Abundance of materials in the Earth's crust[36]

In the cathode, it uses a reagent with the chemical formula NaXO2, where X is one or a combination of transition metals. At the moment, the transition metal that seems to be promising is cobalt. The preference of this metal is related to its success in lithium-ion batteries and, since they are similar in behavior and chemical processes, it crossed to sodium-ion batteries. Not only that, but cobalt is also an element that is present in several processes of clean energy production technologies[26].

In the anode, similarly to li-ion batteries, this technology uses a material that consists of atoms of carbon, usually graphite, due to its readiness and high energy, power density and long cycle life[27]. Other alternatives for the anode consist in the usage of metal oxides. Moreover, these metals belong in the category of transition metals, such as manganese, iron, zinc and vanadium, which have a higher density when compared to graphite (between 7.2 and 9 g/cm^3, while graphite is 2.25 g/cm^3). However, this increase in density results in a larger volume of the battery [37].

This technology is an environmentally friendly alternative to lithium-ion batteries, and has a lower production price per kWh ($40, when compared to $100 for lithium-ion [38]). However, it is not yet ready to be used for public use. Sodium is heavier, has a lower melting point, lower theoretical capacity per unit of weight and volume, lower electromotive force and a larger atomic radius. All of these characteristics, considering that the anode, electrolyte and material of the anode are similar between Li-ion and Na-ion, indicate that this technology has a sluggish performance when compared to its lithium counterpart[39].

Regarding its electrical properties, it has a nominal voltage that is located in the interval of 2.5 and 3.5 V, has a specific energy located between 75 and 150 Wh/kg and has an energy efficiency of 92% and self-discharge rate of 10%. When this battery is operating, its working temperature ranges from -20ºC and 60ºC without any risk of melting or freezing the chemicals within the cell's container [40].

This type of cell has been analyzed to be an alternative to traditional lithium-ion batteries due to their small environmental impact and the low costs of production. Not only that but since they are two metals from the same alkaline group, their chemical behavior is similar. Between the two technologies, the cost of production is significant, as it is visible in table 2.7.

Amp-Hour (Ah)	Cost of typical Li-ion Battery	Cost of typical Na-ion Battery
10 Ah	$100	$70
20 Ah	$170	$120
50 Ah	$450	$300
100 Ah	$500	$350
200 Ah	$1200	$900

Table 2.7: Manufacturing prices of Li-ion and Na-ion batteries for different capacities (Adapted from [41])

These batteries already have the capability to outperform most rechargeable technologies, such as NiMH, Ni-Cd, and are on the same level as LiPo/Li-ion cells. In other words, this technology has the capability to reduce the manufacturing of batteries with toxic chemicals and improve sustainability[41]. Table 2.8 summarizes the characteristics of Na-ion batteries.

Chemistry	Sodium-ion
Nominal Voltage	2.5V - 3.5V
Self-Discharge Rate	10%
Temperature Interval	-20ºC - 60ºC
Production Cost per kWh	$40 - $77

Table 2.8: Sodium-ion Battery Characteristics

Vanadium flow

Flow batteries are a different type of electrochemical energy source. Instead of one container with both reagents on either side of it, these sources use two different reservoirs to store each reagent, which when dissolved in a liquid solution of sulfuric acid, is formed an anolyte and catholyte. These terms are equivalent to saying that the compounds on the anode and cathode are in a liquid state instead of being in a solid state[42].

These fluids travel from the reservoir to a central tank, where the reactions occur, and back to the reservoir. When both liquid reagents are present in the tank, its mode of electricity generation is like any other battery[43]. The schematic of this type of energy source is represented in figure 2.7, as well as the chemical reactions that occur on each side of the central tank.

The advantages of these types of batteries include being able to function for a large period of time, having low recharge time, since its recharging consists of filling the reservoirs with liquid reagents, which also results in long life cycles, and having the capability to use its capacity almost to the fullest. As said previously, these batteries produce energy as long as there are reagents on the central tanks, so they can use all of their battery capacity, since this capacity is directly related to both the central tank and the reservoir's sizes[35].

Nonetheless, one of these batteries' problems is the possibility of occurring cross-contamination of the reagents while they are in the central tank, as it can happen on several other redox examples (iron/chromium, iron/titanium, polysulfide bromium, zinc/chromium). On the Vanadium cells, this type of cross-contamination is non-existent, since both the anolyte and catholyte are made of vanadium ions (on the cathode, V2+ or V3+; on the anode, V5+ or V4+). If one of these ions moves from one side to another, the impact they have on the electrochemical reaction is very low, since this configuration allows cross-contamination up to a limit[44].

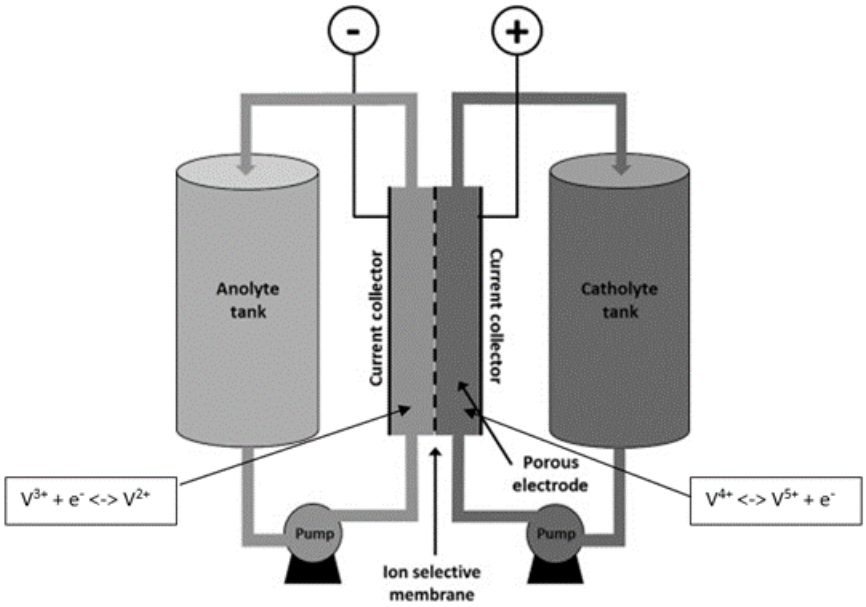

Figure 2.7: Internal characterization of a vanadium flow battery[44]

On one hand, these cells' characteristics include a voltage in the interval of 1.4 V and 1.6 V and a low self-discharging rate. On the other hand, they have a low energy density and specific energy, occupy large amounts of space, have high production costs and they have an energy efficiency of up to 85%. Despite this last value being greater than most common battery technologies (Lead-Acid, NaS, Ni-Cd, NiMH), they are outclassed by li-ion batteries when considering individual cells. However, from the point of view of a large system, these cells can potentially surpass li-ion due to the reduction of working temperature and, in consequence, their efficiency. Due to their mode of operation and significant dimensions, they can be used alongside renewable energy systems, or as an uninterruptible power supply[45].

While this battery configuration is more efficient regarding the prevention of leakage from the electrodes' reservoirs, its components include sulfuric acid, a powerful acid that can cause a significant impact on both the environmental and individual health[17]. Table 2.9 summarizes the characteristics of vanadium flow batteries.

Chemistry	Vanadium flow
Nominal Voltage	1.4V - 1.6V
Self-Discharge Rate	0%
Temperature Interval	-20ºC - 60ºC
Production Cost per kWh	\$40 - \$77
Disadvantages	- Needs to be refuelled to be used - Uses toxic materials (Sulfuric Acid)

Table 2.9: Vanadium flow Battery Characteristics

2.2 Battery Analysis

The major benefit of portable power sources, such as batteries, resides in the ability to move between places with an electronic device without it being constantly connected to the power grid. With the usage of secondary batteries, this situation is more beneficial due to the possibility of recharging the battery whenever it is discharged when compared to primary batteries, which cannot be recharged. Nonetheless, batteries do not remain in the same condition over time and after each charging cycle. In these cases, one must be aware of the battery's behavior (reduction of autonomy, chemical leaks to the outside, battery swelling), or its State of Health (SoH). To estimate the state of health (SoH) of a battery, several techniques assist in this task. They can either result from measurements of the system in question or use datasets with values adequate for the analysis. In this section, it is going to be presented several techniques that allow the analysis of the internal behavior of the cell.

2.2.1 Direct Analysis

The methods presented in this section reside in the analysis of information that is collected via direct measurements (such as voltage or impedance measurements). These approaches often generate values assisted by the use of devices such as multimeters.

Voltage Measurement

A simple approach regarding voltage analysis is the measurement of a cell's voltage in an open circuit and observing its behavior over time. However, this procedure does not describe the precise status of the battery itself, whether its State of Charge (SoC) or its state of degradation (or State of Health (SoH)). While battery manufacturers give a voltage interval, and its thresholds can result in the estimation of the SoC (when the battery's voltage coincides with the upper limit, the battery is fully charged - SoC is 100%; when the battery's voltage is equal to the lower limit, it is discharged - its SoC is 0%), the values that are between these thresholds often remain in the same voltage value, which matches with the value of nominal voltage [46]. This can be visible in figure 2.8, where, despite the variation of the voltage being between 1.4V and 1.0V, for a large time of its discharge operation, it settles on the voltage value of 1.2V (nominal voltage), thus making it difficult for the estimation of SoC.

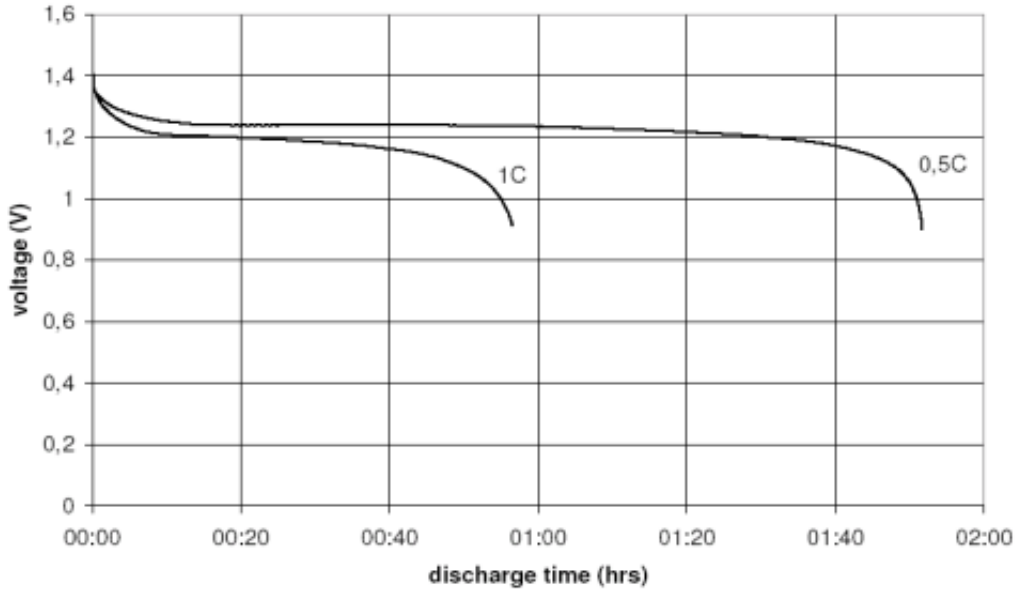

Figure 2.8: Voltage discharge behavior for one NiMH cell, during fast and normal discharge procedures (plots of 1C and 0.5C, respectively). **C** represents the nominal capacity of the battery [47]

Charging/Discharging Curve

While the battery does have voltage and can be used as a voltage source, the internal reaction of the chemicals results in the generation of electrons that dislocate from the battery to an external circuit. Since the previous method focused primarily on the analysis of the voltage values, the analysis of charge and discharging curves allows for a better study of the cell when submitted to certain conditions of current and voltage supply. Nonetheless, this test's configuration has to be made with the assistance of the manufacturer's information, since it subjects the battery to a certain amount of stress (due to voltage and current limitations imposed by the battery tester). This process starts with the tester in Constant Current (CC) mode, charging/discharging the battery until it reaches the pretended voltage value. After it hits the expected value, the instrument enters in Constant Voltage (CV) mode, where the current value gradually decreases until it reaches a low current value (usually definable by the user).

If these stress factors (voltage and current limits) are set to a value much higher than those specified by the manufacturers, the battery can have behavior harmful to the battery, such as battery swelling (the internal chemical reactions of the battery occur at a faster rate, resulting in a rise of temperature which, when exceeded, expands the internal components of the battery and, consequently, its external casing) [46]. The sample rate also has an impact on this test. When using a low value, fewer readings are going to be performed by the tester, thus reducing the accuracy of the plot drawn from these readings. If the sampling rate has a higher value, there is a

higher quantity of readings from the tester, increasing the accuracy, but the size of the final data file is significantly higher when compared to a lower sample rate.

Electrochemical impedance spectroscopy (EIS)

An alternative to the charge/discharge performance analysis consists in the implementation of an electrochemical impedance spectroscopy, a process that analyses the battery behavior based on its internal chemical reactions and respective impedances [48].

This test functions by applying an excitation signal of reduced amplitude, in this case a voltage signal to an electrochemical cell, like a battery. The cell generates an output signal of reduced amplitude (in this case, electrical current). However, the output signal differs from its input by being shifted in phase. This shift is a result of the internal components of the battery [49]. As is visible in the upper part of figure 2.9, the equivalent electric circuit has resistive and capacitive components. Capacitive components have an impact on the phase shift since they generate a negative phase in the output signal) [50].

After the analysis of both the input and output signals, the internal impedance of the battery can be calculated with the following formula:

$$Z(j\omega) = \frac{E(t)}{I(t)} = \frac{E_0 \sin(2\pi f)}{I_0 \sin(2\pi f + \phi)} \tag{2.4}$$

where **f** represents the frequency of the input signal, **E(t)** and **I(t)** represent, respectively, the input voltage and output current signals, and $\boldsymbol{\phi}$ represents the phase shift of the current signal from the voltage signal.

Since the impedance value is not constant due to the continuously altering values of current and voltage, its representation is made by a pair of complex numbers (resulting from the phase shift) written in the polar form ($Z = Z_0(\cos\phi^* + \sin\phi^*)$), whose phase ϕ^* has a symmetric value than that of the current ($angle(Z) = angle(E) - angle(I) <=> \phi^* = -\phi$). The visualization of the data can be observed by drawing a plot of the real part of the impedance (Z') in function of its imaginary part (Z"), as can be visible in figure 2.9.

2.2.2 Indirect Analysis

The methods presented here are used primarily without the assistance of any measurement devices, since the data it uses originates from previously created datasets. They are procedures that are more demanding on a computational level due to having to run several hypotheses in order to estimate the one that is most fit for the situation. Some examples are optimization algorithms, equivalent electrical circuit modeling and machine learning.

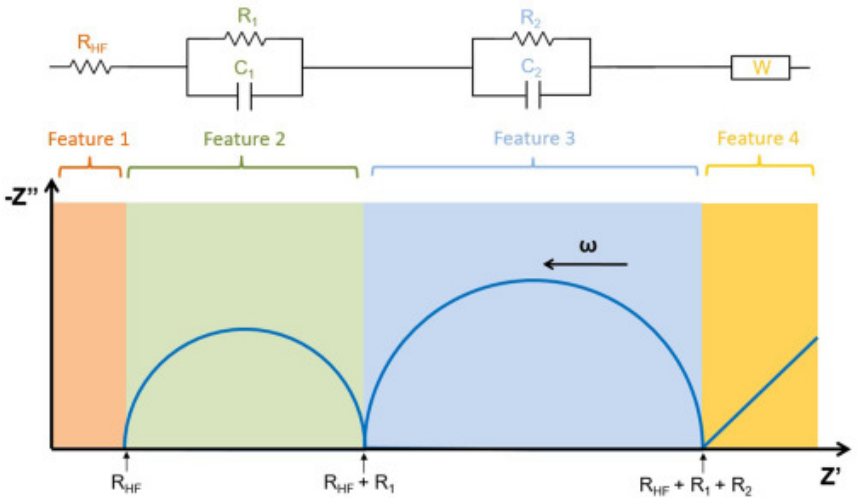

Figure 2.9: EIS of a battery and respective equivalent circuit[49]

Optimization Algorithms

One way to optimize the estimation of model parameters is by using optimization algorithms. They scour through the given datasets to discover the optimal or most adequate value. With small datasets, it is a quick process. However, with large sets of data, this procedure can last a long time while using a lot of processing power. One such approach is the genetic algorithms, which use processes inspired by the evolution and natural selection of genes to select the ones that are most fit for the problem at hand [46].

Another approach is the Particle Swarm Optimization (PSO), an algorithm based on the social interaction between birds where, in a given set of data, each one of the values is responsible for discovering the most optimal values. Unlike genetic algorithms, whose selection of the optimum value is based on natural selection (survival of the best gene that is most fit for the characteristics defined), PSO's selection method is based on the social behavior of birds, where each one of the particles interacts with each one of the remaining on a search space. During these interactions, the algorithm sorts the particles by fitness values (how suited they are for the search space) [51].

Equivalent Electrical Circuit Modelling

Another method that relies on data is the development of an equivalent electrical circuit of a battery. Despite differences between chemistries, it can be used to display a graphic representation and analyze its performance over time. Moreover, this procedure can only be used in conjunction with other methods that allow the estimation of the model parameters (optimization algorithms, curve fitting, charge/discharge

plotting). One example of an equivalent electrical circuit is presented in figure 2.10[46].

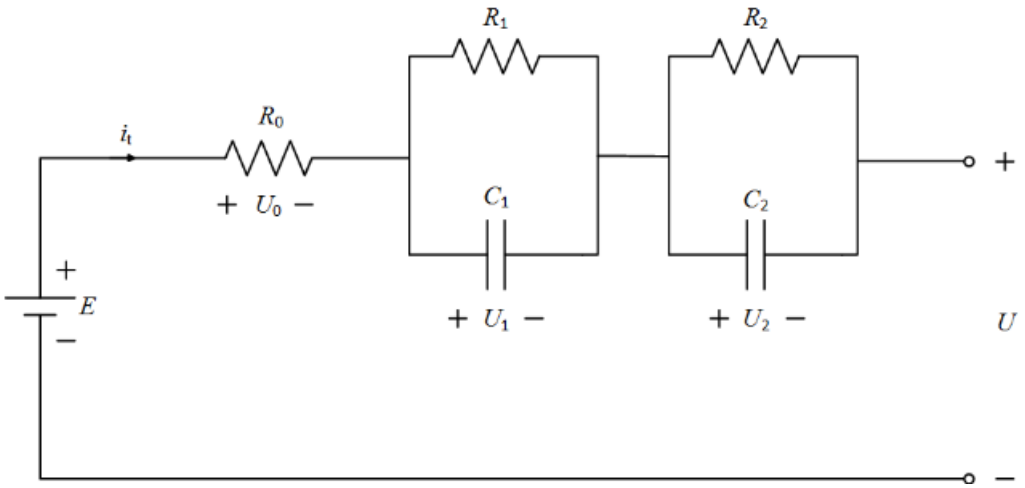

Figure 2.10: Equivalent circuit of a battery [52]

This procedure is commonly used due to its lower requirements regarding computational power (when compared to other alternatives within this group) and capacity for real-time analysis of the behavior of the battery. The model shown in figure 2.10 is the most used when representing this behavior due to its RC pairs, which induce a phase delay caused by the use of capacitive components (hence the reversion of the imaginary impedance on the EIS in figure 2.9). Moreover, this method can only be performed alone when it has a set of data regarding its behavior during charge/discharge processes. It is commonly associated with other processes responsible for the collection of the values regarding the performance of the battery (current, temperature, voltage). This gathering is usually made with the assistance of Kalman filters, Machine Learning (ML) algorithms or the analysis of charge/discharge curves[46].

Machine Learning

Several computational algorithms such as genetic algorithms and artificial intelligence are based on biological events. While genetic algorithms are based on human evolution, artificial intelligence algorithms (machine learning, deep learning) are based on the human brain. Speaking particularly of the second type, computers acquire intelligence by learning processes from data provided by the programmer.

In order to function as intended, machine learning requires a large amount of data. It can come either from experiments or from datasets. For the estimation of the battery's electrochemical state, it is necessary to extract the information necessary for its evaluation and perform its measurement. Normally, the values that are frequently used are current and voltage. However, these values offer a rather simple approach to the analysis of the battery's performance from an electrical

point of view. Therefore, the measurement of different parameters leads to the development of a more complex and, simultaneously, more exhaustive performance analysis.

Chemali et al[53] discovered that, on this subject, the typical dataset consisted of ideal SoC values and a vector which included all of the inputs at a given instant. In this case, this input vector consists of the measurement of the voltage, temperature, average current and average voltage in an instant $\mathbf{t}$. The introduction of the average values of voltage and current is justified by the authors as being more efficient from a computational point of view, as well as less demanding on the quantity of memory that is required by the algorithm. In order to make the network training more accurate, this framework uses backpropagation, meaning that it can update the weight of the input values at the end of the training epoch, when all the data present in the dataset has been used. This training process can have several epochs, which result in a better accuracy of the neural network but a longer computing time, since it takes longer to train the network.

2.2.3 Hybrid Analysis

These processes tend to use direct measurements, as well as digital processing of these values to offer a higher degree of accuracy, since they use both direct and indirect data. One of these processes is the Kalman filter.

Kalman Filter

Devices such as multimeters and sourcemeters can implement measurements of several circuit parameters, such as voltage, current, resistance and temperature. However, these devices are not fully accurate due to the lack of precision of both the components and the device itself. So, manufacturers usually specify the degree of accuracy that the equipment is subjected to.

One of the ways to reduce possible measurement errors, as a consequence of the existence of electrical noise, is with the assistance of prediction algorithms, such as the Kalman filter. This algorithm reduces the measurement error, thus increasing the measurement precision.

Before the execution of the algorithm, one must make some considerations regarding the initial guess. More specifically, about the estimated uncertainty and state of the system. This step is only meant to be executed once in order to give a basis for the system's dynamic equations. At the end of this step, since the values used are considerations regarding the state of the system (and not real values directly retrieved from the system), these values stay the same, and become estimations for the next iteration of the system, this time applicable with the system's equations.

After the initialization, the system is set to start working. Here, the algorithm will consider measurements of the system's variables (for electric circuits, this can be current, voltage or resistance) made from a device with a certain measurement uncertainty. These values will be taken into consideration for the beginning of the system. At this stage, with the dynamic system up and running, the measurement values are those that are acquired by measurement devices, and the measurement error is that of the device. When using this technique, there are 3 formulas that form the basis of the Kalman filter: the Kalman Gain (represents the weight of the difference between the measurement and the estimated value, obtained from the predicted value in the previous instant. It is present in equation 2.5), estimation of the current state (equation 2.6) and estimation uncertainty of the system (equation 2.7).

$$\text{Kalman Gain} = \frac{p_{n-1}}{p_{n-1} + r_n} \tag{2.5}$$

$$\hat{x}_n = \hat{x}_{n-1} + \frac{1}{n} * (z_n - \hat{x}_{n-1}) \tag{2.6}$$

$$p_n = (1 - K) * p_{n-1} \tag{2.7}$$

where $\hat{\mathbf{x}}$, $\mathbf{p}$, $\mathbf{z}$ and $\mathbf{r}$ represent the estimated system state, estimate error, measurement and measurement error, respectively for the current instant of time (**n**) or the previous instant (**n-1**). After performing these calculations, in the following iteration, the values calculated previously will be the base for the calculation of new estimated values. This mathematical cycle corresponds, in figure 2.11, to a loop between steps 1 and 3 (measurement, update values and prediction of values in the next instant).

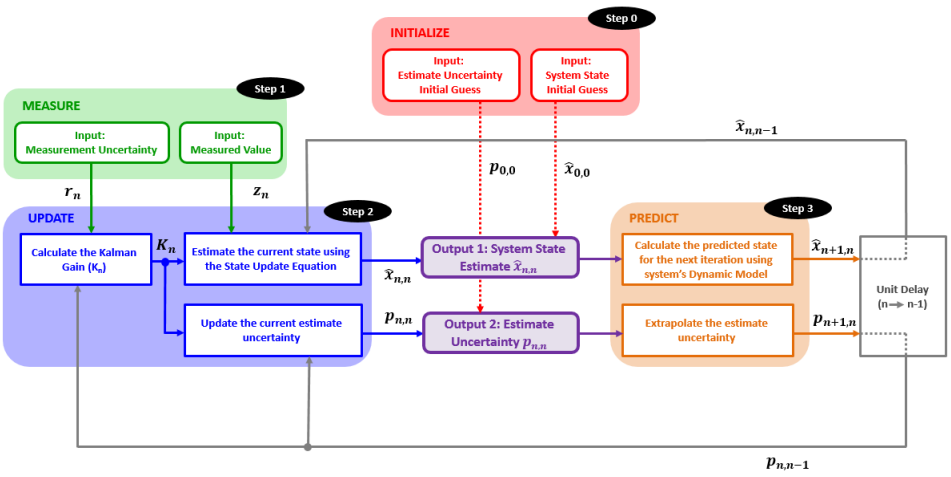

Figure 2.11: Block diagram of the Kalman Filter [54]

Spagnol et al [55] use this method, alongside the equivalent electric circuit procedure, to estimate the SoC of a lithium-ion battery. For the development of the

equivalent model, shown previously in figure 2.10, there were several mechanisms that allowed for the implementation of the model.

1. Estimation of the Open-Circuit Voltage (OCV) - the authors charged or discharged the battery with a step of 1C, where C is the nominal capacity of the battery, with variable duration. The variable duration of the step was chosen due to the different behavior of lithium-ion chemistry during its charging or discharging process, alternating from non-linear to linear and back to non-linear behavior, according to figure 2.12.

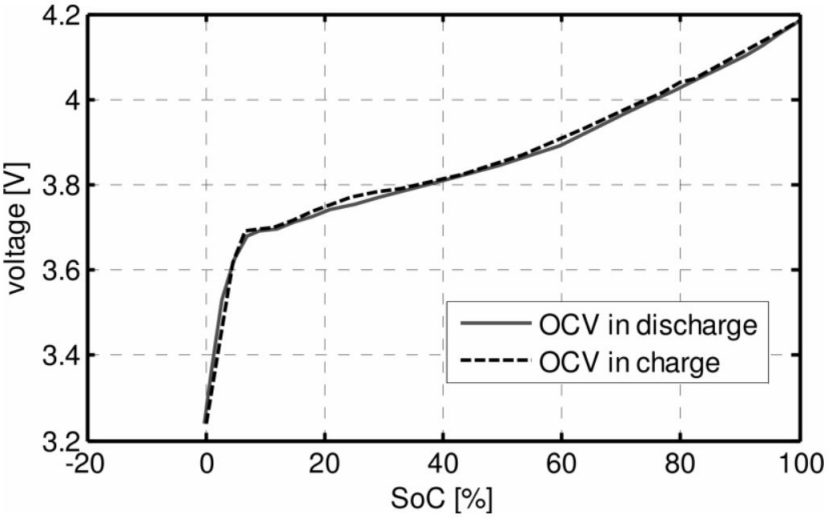

Figure 2.12: OCV estimation during discharge (continuous line) and charge (dotted line)[55]

2. Estimation of the resistance R0 - This estimation is made through the current pulses observed during the analysis of the lithium-ion battery's performance, represented in figure 2.13. Both graphics have marked points, which represent the interval of current and an interval of voltage (on the upper and lower plot, respectively) that the resistance has an effect. From those values, and applying Ohm's Law, it is obtained the value of the resistance R0 in that instant. By summing these values over time, this parameter is more representative of the behavior of this technology over time.

3. The calculation of the remaining parameters (R1, C1, R2, C2) is made through the equation of the electrical mesh, indicated in equation 2.8.

$$(-v(t) + v_{OCV}(SoC) - R_0 i(t))/i(t) = \frac{R_1}{1 + sR_1C_1} + \frac{R_2}{1 + sR_2C_2} \tag{2.8}$$

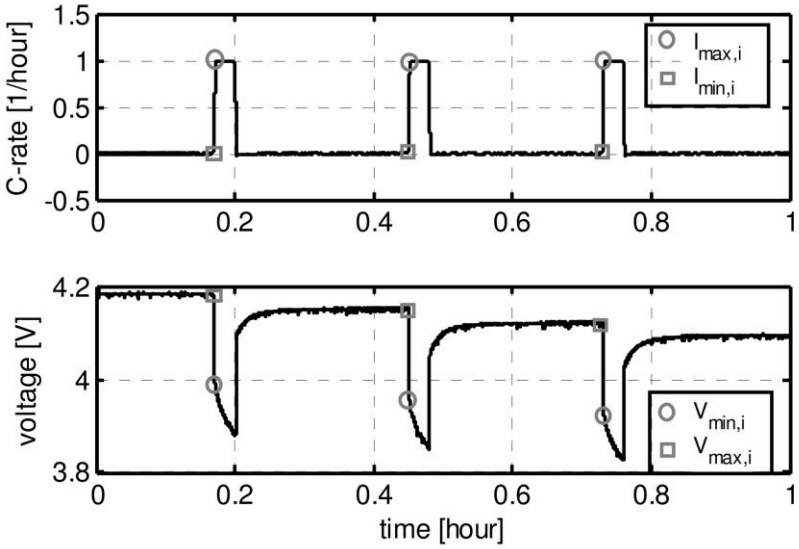

Figure 2.13: Evaluation of R0 over time[55]

2.3 Decision Support Systems

2.3.1 Support Vector Machine (SVM)

The SVM is a supervised parametric algorithm used for either regression or classification problems. It works on the principle of Structural Risk Minimization (SRM) - creating several variations of the model in order to find the one with lower empirical risk or risk of overfitting [56]. For the purpose of this report, the approach that is going to be further analyzed is SVM applied to classification problems or Support Vector Classifier (SVC), as a means of comparison to another similar approach, described in the next section.

In order to use this algorithm, one must define the mathematical model that is implemented for the data separation (and consequent class generation), often called the hyperplane. Depending on the diversity of information used for training, the hyperplane can have various forms and equations, such as lines, parables and circles. After the hyperplane is selected, the user introduces the set of values that are going to be used as the training set for the algorithm. Once the values are inserted, the algorithm attempts to separate them into various classes. The location of the hyperplane is not an arbitrary one. It is positioned so that it has the same distance between classes' edges (called support vectors), in order to provide an equal margin between each class. This explanation is represented in figure 2.14.

This algorithm provides a high degree of accuracy due to the existence of a reference for the separation of the data. Additionally, this algorithm generates an abstraction (list of essential characteristics or patterns) of the dataset, thus reducing the memory required for the storage of the model. However, the generation of an

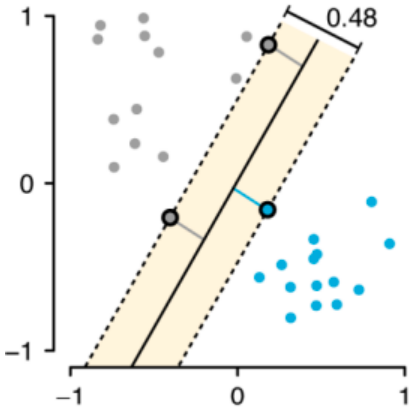

Figure 2.14: SVM Class Separation[57]

abstraction can contribute to a long training period, since it has to analyze each point individually in order to extract the fundamental aspects of the data [58].

Moreover, this algorithm can also be used for regression problems. Chen et al [59] used this algorithm to calculate the SoH of Li-ion batteries. This procedure is derived from the charging/discharging of 2 batteries. The values obtained are voltage, current and the time required to reach the upper or lower cutoff voltage (in the case of charging or discharging, respectively). With these values, the authors calculated three variables required to track the SoH variation. From the voltage signal obtained through measurements, its energy was calculated for the operation at hand (charge or discharge). From the current values obtained, the battery capacity was estimated. Finally, the authors also recorded the time it took for the battery to reach the upper and lower interval of voltage[59].

2.3.2 k-Nearest Neighbors (kNN)

The KNN is a supervised nonparametric algorithm often used for classification problems that do not require the existence of any kind of mathematical model, instead learning from the input information.

The way this algorithm works is that it generates a neighborhood with the training data as points in this neighborhood and, given values by the user, it checks the distance between the point created with the user's data and each of the neighbors. After the calculation of the distance, the algorithm returns the characteristics of the nearest neighbors. The quantity of the neighbors that the algorithm selects is dependent on the value the user gives (represented by the parameter k). The graphical representation can be observed in figure 2.15

There are several distance metrics used in this algorithm [61]. The metric commonly used is the Euclidean Distance, a metric that calculates the distance as the square root of the sum of squares of the difference between the cartesian coordinates

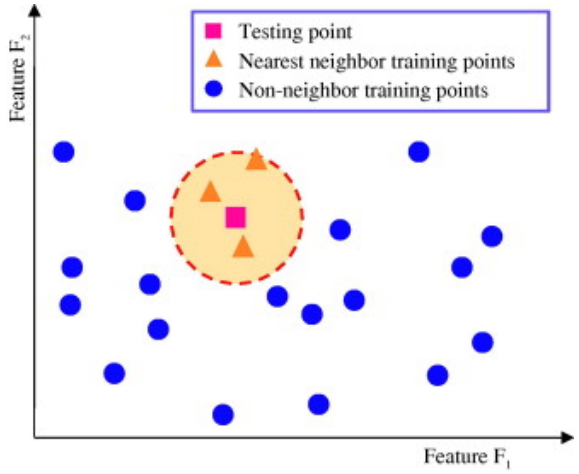

Figure 2.15: KNN classification [60]

of the data points. Despite the existence of this metric, another alternative metric resides in the use of the Manhattan Distance, whose distance is calculated by the sum of the absolute differences of the cartesian coordinates of the points (otherwise known as taxicab geometry, since its trajectory is made accordingly to one of the cardinal directions: North, South, East, West). When dealing with high-dimensional data, it is advisable to use the Manhattan metric instead of the Euclidean [61]. These equations are written below in equations 2.9 and 2.10, respectively.

$$Euclidean\ Distance = \sqrt{\sum_{n=1}^{N}(x_i - y_i)^2} \tag{2.9}$$

$$Manhattan\ Distance = \sum_{n=1}^{N}|x_i - y_i| \tag{2.10}$$

This algorithm uses an instance-based learning mechanism, meaning that it does not create an abstraction of the data like other machine learning algorithms such as SVM. Instead, it pinpoints the data's location in a referential. Additionally, its mode of operation is simple to figure out since it requires basic mathematical concepts such as geometrical distance (distance between two points in a referential) instead of more complex operations such as integration or differentiation. Its implementation can be present in medicine, for the prediction of medical conditions based on the history of previous patients with similar symptoms, or in the financial sector, for the prediction of the best time to buy stocks based on past history of the stock and current factors external to the stock market [62].

However, the simplicity of using this algorithm is also one of its disadvantages. Since it does not develop an abstraction like other algorithms such as SVM, the KNN model's size is significantly larger, resulting in the allocation of a large amount of memory that is proportional to the size of the dataset[63].

Similarly to SVM, the KNN can also be used for regression problems. Hu et al [60] used KNN, alongside with the particle swarm optimization algorithm, to estimate the capacity of lithium-ion battery. For this article, the key values used were voltage, current and capacity during the charging of the battery, specifically the voltage values corresponding to the start and end of charging, the capacity when is being supplied in Constant Current (CC) and Constant Voltage (CV) modes, and the current when the voltage reaches its maximum voltage. The features used in this article are described in figure 2.16.

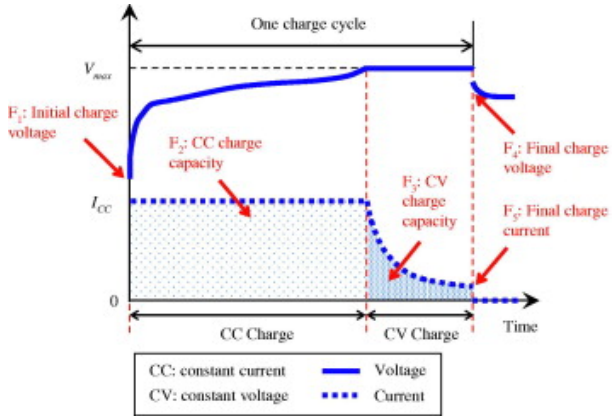

Figure 2.16: Charging Features [60]

Given these features, they are introduced into the KNN as inputs to generate a regression model whose output is battery capacity. Afterward, with the assistance of the particle swarm algorithm, the weights corresponding to each of the input parameters, indicated in the previous paragraph, were modified in order to reduce the Root Mean Square Error (RMSE), the error between the regression model created and the measurements taken.

2.4 Existing battery datasets

In this section, some battery datasets are presented, describing their contents and papers where they were used. These datasets only consist of data retrieved from lithium-ion batteries, as no information regarding public datasets for other chemistries was found.

2.4.1 Toyota Research Institute (TRI)

This open-access dataset consists of 124 Li-ion batteries with cycle lives ranging from 150 to 2300 charging-discharging cycles. These batteries were tested in a controlled environment with a temperature of 30ºC, with different charging conditions but identical discharging conditions [64].

This dataset is mainly used for the SoH or SoC estimation. In the article written by Chen et al[65], this estimation is made of two steps, collection of data and prediction. To perform the data collection, batteries were subjected to Empirical Mode Decomposition (EMD), which decomposes a signal into several components. For this case, charging and discharging curves are the signals and their components are voltage, capacity and current, as well as the existence of a capacity residue, resulting in a slight spontaneous increase of capacity (usually in the order of tenths of mAh) observed and included in the analysis to increase accuracy.

The prediction of the SoH itself is made with the assistance of two algorithms. One of these algorithms is the Autoregressive Moving Average (ARMA) model. This model is composed of two different models, an autoregressive (AR) and a moving average (MA), resulting in more accurate prediction results based on past samples. However, the use of this algorithm requires a high level of data stability, so a differential equation is applied to the input signal to stabilize it and, after this stabilization, its samples are inserted into the algorithm. In addition to the ARMA model, the authors also used a recurring NN to predict the capacity residue of a battery. Using these two algorithms simultaneously, the information originating from this dataset was used for purposes of validation of the model.

2.4.2 NASA

The North American Space Agency (NASA)'s Prognostics Center of Excellence (PCoE) experimented in 50 Li-ion batteries. These experiments consisted of three different methods of analysis, each with their own values and approaches [66].

The first experiment is the charging of the cell, which generates the values of current and voltage in both the charging circuit and the battery terminals, as well as the battery's temperature. This process consists of the supply of a constant current value of 1.5A until the battery voltage reaches 4.2V. When this voltage is reached, it remains constant and the current starts dropping until it reaches 20mA. The parameters within this procedure are indicated in figure 2.17.

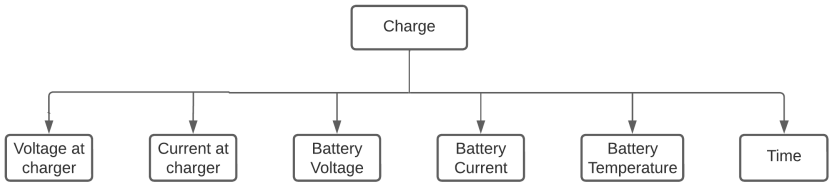

Figure 2.17: Charging parameters of 18650 Li-ion battery (values extracted from [66])

The second experiment is the discharge of the cell, which generates numbers regarding voltage and current at the battery's and at the load's terminals, as well

as the battery's temperature and capacity at the end of the discharge. This type of assessment consists of supplying a constant current of 2A until the battery reaches its cutoff voltage, stated by the manufacturer and, for the case of li-ion batteries, usually is about 2.7-3V. The parameters within this procedure are indicated in figure 2.18.

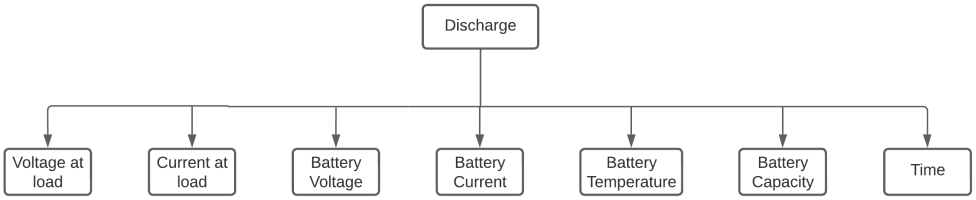

Figure 2.18: Discharging parameters of 18650 Lithium-ion battery (values extracted from [66])

The third experiment is the analysis of the internal impedance of the battery, performed by a frequency sweep between 0.1 and 5000 Hz. This variation of frequency allows for the internal chemicals to react to the excitation signal, thus having a reaction that impacts the internal impedance. However, some components of the battery have a more significant reaction when subjected to higher or lower frequencies. The parameters within this procedure are indicated in figure 2.19.

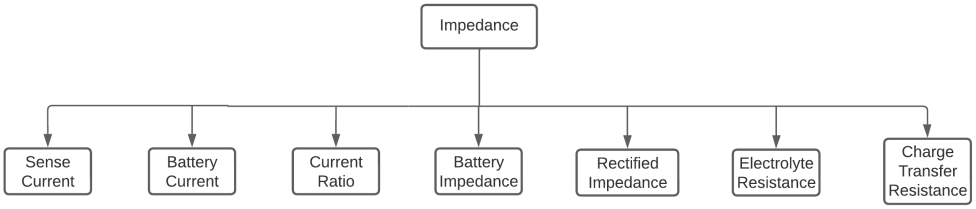

Figure 2.19: EIS parameters of 18650 battery (values extracted from [66])

Ma et al[67] used this dataset in order to predict the Remaining Useful Life (RUL). For this prediction, the authors used two techniques. One of them is the False Nearest Neighbor (FNN), whose purpose resides in the analysis of the nearest neighbors when the data dimension shifts. If the dimension shifts and a neighbor is no longer a neighbor, it is considered as being a false neighbor (FN). Another technique resides in the use of two neural networks combined (CNN – Convolutional NN, and LSTM – Long Short-Term Memory), resulting in one hybrid neural network. This article uses battery capacity values over several cycles to predict the End of Life (EoL) of the cell. For this case, since it used the NASA Prognostic Center of Excellence (PcoE) dataset, the criteria for the reach of EoL resides in the decrease of capacity of 30% [67].

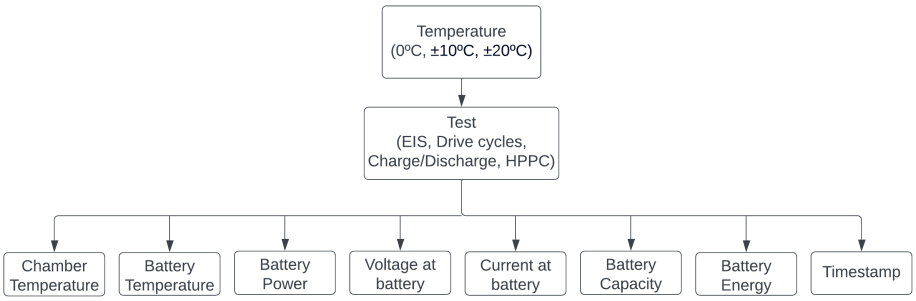

Figure 2.20: Structure of the University of Wisconsin-Madison's dataset [69]

Additionally, Jo et al[68] used this dataset for the training of 3 different neural networks (Feedforward NN, Convolutional NN and Long Short-term Memory) and observed their performance when predicting the SoH of the battery using values regarding current, voltage, temperature and capacity [67].

2.4.3 University of Wisconsin-Madison

Created by Dr. Phillip Kollmeyer [69], this open-access dataset consists of the testing of one Li-ion battery under different conditions of temperature. The testing profiles were made with the assistance of a Digatron Firing Circuits Universal Battery Tester and several of the profiles designed were the HPPC (Hybrid Pulse Power Characterization), which consists of the generation of pulses of 1C of amplitude with different duty cycles and resting periods (time between pulses), and EIS (Electrochemical Impedance Spectroscopy). The file structure of this dataset is represented in figure 2.20

Zhao et al[70] used this dataset to train two Recurrent NN (RNN) for the estimation of SoH. While both networks use values of voltage and temperature, one also uses current and capacity values and the other uses power and energy values. These last two values are calculated analytically (power is the product of current and voltage, and energy is the product of capacity and voltage).

When estimating the SoC, Chemali et al[71] use an LSTM neural network trained with values from this dataset. These input values for the network are battery voltage, current and temperature, and the output is the SoC.

2.4.4 Center for Advanced Life Cycle Engineering (CALCE)

This free-access dataset [72] comprises information from 5 different types of batteries. While all tested batteries use the li-ion technologies, their testing profiles differ. Some of them were used to observe the open-circuit voltage, using low current (discharging of the cell until a certain value has been reached) or incremental current

(similar to low current, but it includes a resting period every 10% of the battery's maximum SoC. Additionally, another set of batteries is subjected to a diversity of stress tests.

Zheng et al[73] use this dataset to verify the influence of different OCV tests and later to create an electrical model. This is done by creating a look-up table that shows the relationship between OCV and SoC. The authors then subjected the battery to a Dynamic Stress Test (DST). This is a dynamic discharge regime consisting of several power steps with random amplitudes to estimate the passive components of the circuit. Finally, the authors use a curve-fitting algorithm to estimate the best values that best represent the battery's curve expression to derive the model's expression. An Unscented Kalman Filter (UKF) was used for real-time estimation of the SoC to obtain the most accurate results.

2.4.5 Wang et al

This dataset [74] uses 2 different testing subjects (a lithium-ion battery and an ultracapacitor, used as a smaller backup battery for whenever it is required an additional energy surge). These subjects were tested according to Dynamic Stress Test (DST) and Urban Dynamometer Driving Schedule (UDDS), tests that are mainly used for the testing of batteries used for powering an electric vehicle. For the tests at hand, since its target is only to visualize the performance of the battery and the ultracapacitor when used in an electric vehicle, the measurements only consist of the voltage and current. The positive and negative values represent, respectively, the charge and discharge operations. The parameters within this procedure are indicated in figure 2.21 and 2.22.

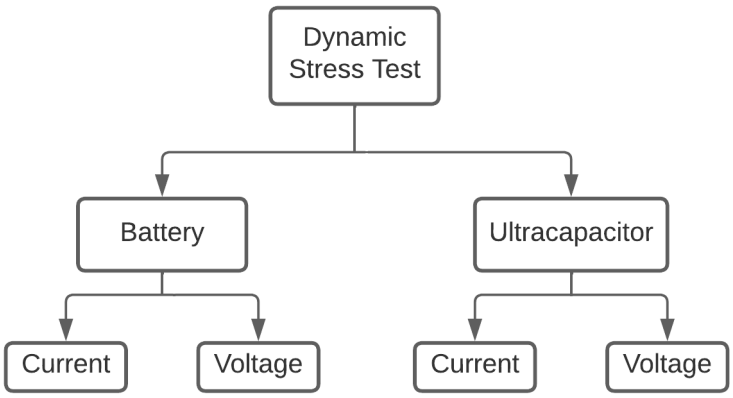

Figure 2.21: DST test parameters [74]

Li et al[75] developed a cloud-based battery management system (BMS) with a data-cleaning approach depending on a Machine Learning algorithm. Inside the

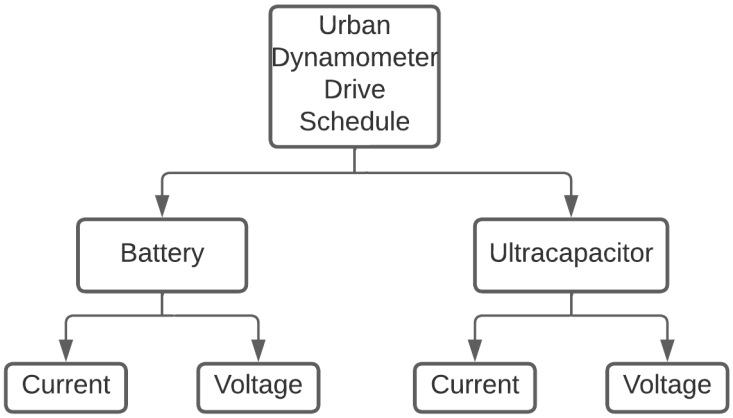

Figure 2.22: UDDS test parameters [74]

cloud, the target parameters' values are stored for the generation of the battery model. This article uses this dataset for the estimation of the SoC and the voltage at the battery's terminals. This voltage, alongside the BMS present in the vehicle, is compared to the voltage of the real battery so that, in the existence of a fault or discrepancy of values, the battery is removed from the car to be diagnosed.

Chapter 3

Development of the project

This chapter describes the implementation of a decision support system for battery selection. Based on a set of characteristics of a given IoT application, this system should identify the most appropriate battery. To do this, it was necessary to identify which battery chemistries to analyze (sub-chapter 3.1), identify which characteristics to use and acquire the respective data (sub-chapters 3.2 and 3.3). After acquiring the data, the algorithm was trained (sub-chapter 3.4) and then validated with an example (sub-chapter 3.5).

3.1 Hardware and Software Requirements

For the purpose of this work, four battery chemistries were selected: Ni-Cd, NiMH, LiPo and Li-ion. Emerging technologies were disregarded due to either market unavailability (Na-ion) or inadequacy due to issues regarding its dimensions (Vanadium flow) or thermal maintenance (NaS).

Another requirement that was taken into consideration was the battery's suitability for IoT devices. For this motive, the main focus of the selection consisted in the arbitrary selection of batteries with different capacities (in this case, 0.7Ah, 1.3Ah and 2Ah), as well as different chemistries. For the different chemistries, 2 batteries of each chemistry (Ni-Cd, NiMH, Li-ion, LiPo) were selected which resulted in different discharging duration. Moreover, there is a difference between these chemistries' nominal voltage (Li-ion and LiPo have 3.7V, while NiMH and Ni-Cd have 1.2V). In order to discard voltage as a variable between batteries, for the data acquisition 3

individual cells in series of each of these chemistries were used (thus making a total of 3.6V and, as a consequence, discarding voltage as a differentiating parameter).

For NiMH and Ni-Cd batteries, 3 individual cells were used in series. This selection has been made so that the 4 chemistries can be compared in the same range of values (since Li-ion and LiPo batteries have a nominal voltage of 3.7V).

Since each battery has a certain number of characteristics, such as chemicals and dimensions, its selection can become troublesome due to a large number of variables. The datasets mentioned in sub-chapter 2.4 show a variety of procedures that can be used to observe battery behavior (in that case, only Li-ion batteries), ranging from OCV curve analysis to more complex procedures such as EIS. While these methods can be applied to any battery chemistry, the process used to acquire data to the dataset was the analysis of charge/discharge curves, as it provides accurate readings for detailed analysis. However, the use of this method submits the battery to a stress test, making it time-consuming while having unwelcoming results such as swelling, overheating and short-circuiting. The selection of the battery's capacity was arbitrary, the criteria being that the cells could be discharged on one day and charged in the next one as well as being light for being fit in small devices.

For the acquisition of the data, two devices were used: the Keithley 2281S-20-6 and the Keysight 34410A. The first device is presented by the manufacturer as a "battery simulator" and can be configured for the execution of three different operations[76]:

- Supply power to an external circuit.
- Simulate the working principle of a battery.
- Test a battery by performing charging/discharging cycles. Data acquisition was achieved using this function

The second is the multimeter, a device able to accurately measure both instant voltage, resistance and current in real time. This device is going to perform temperature measurements with the assistance of an external temperature probe. This probe, taking into account the specifications of the multimeter as well as its compatibility with temperature measurement in LiPo, Ni-Cd and NiMH batteries, is a Resistance Temperature Detector (RTD). However, Li-ion batteries are manufactured with a protection circuit (to prevent voltage and current spikes), which includes a Negative Temperature Coefficient (NTC). The difference between these two probes resides in the materials used for their manufacturing, with RTD being made of solid metal (has better thermal conductivity but is more expensive) and NTC being made from an epoxy (has lower temperature conductivity but is less expensive) [77].

Both devices were then connected to a computer where all acquired data was stored and processed. From these devices, only the battery tester offers internal data storage limited to 2500 measurements. These measurement samples were fetched using Standard Commands for Programmable Instruments (SCPI), a standard created for the development of a common interface between computers and test instruments. Its syntax is made of one or more ASCII strings (depending on several commands sent at once) and is used alongside several Test Applications Environments, such as LabVIEW, MATLAB, Microsoft Visual Studio or Agilent VEE. This standard is hardware-independent, and it works with numerous communication protocols such as GPIB, RS-232, VXI or LAN networks [78].

When it comes to communication between the devices and the computer, while the standard that is going to be used is SCPI, the script that establishes the connection and data processing between the two devices and the machine is going to be written in Python. This programming language allows for the addition of extra features and functions through the installation of packages. In this project, some of the most predominant are going to be NumPy, Pandas, Matplotlib and PyVISA. Although the first three are used in situations of data analysis and data exhibition, PyVISA has an entirely different purpose. The usage of this package is given by its capacity to simplify the communication configuration between measurement instruments and remote machines. This package uses the Virtual Instrument Software Architecture (VISA) specification, which allows for its implementation on most programmable devices due to its compatibility with a large variety of interfaces, such as Ethernet, USB, GPIB, RS232 [79].

3.2 Data Acquisition

Once the measurement equipments are connected to the computer, the following step is the configuration of the battery tester to charge or discharge the battery. This configuration is made with SCPI syntax and transmitted with the assistance of the read(), write() and query() functions included in the PyVISA library. Given that the battery tester will be programmed for its testing function, all that remains is to configure this device specifically for the battery chemistry at hand. The main characteristics that are going to be configured are described as follows:

- Cut-off and over-protection voltage - Respectively, the cut-off voltage and the voltage at which the device enters safe mode and stops the process. These parameters can be configured with the SCPI commands.
- Current Limit - The minimum current value at which the charge/discharging process stops.

- Charging current (for the battery charging) - Current that will be sent to the battery. When discharging, this value is capped at 1.25A.
- Sampling Interval - Period at which a sample is generated.

After the testing variables are configured according to the manufacturer's data sheets, all it is left to do is start the execution of the process. Depending on the cut-off voltage that is inserted, the tester can interpret it as being a discharge or a charge of the battery. The data that is extracted either from the battery tester or from the multimeter are stored in a list, alongside a timestamp at which the measurement was performed, inserted after the measurement with the assistance of the function time, part of the library with the same name. After the list is created with the value of voltage, current, capacity, timestamp and temperature, it is stored in a CSV file to simplify future analysis and data extraction (see code in appendix A). An example of curves for NiMH batteries is visible in figure 3.1.

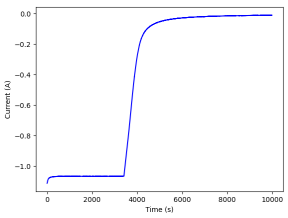

(a) Continuous current analysis

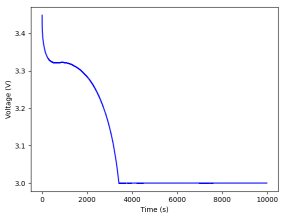

(b) Continuous voltage analysis

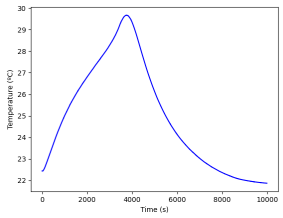

(c) Continuous temperature analysis

Figure 3.1: Some experimental data from NiMH batteries

3.3 Dataset Building

As explained previously, the acquisition of values is made with the assistance of SCPI commands and PyVISA for performing queries to the measurement devices. Data transmission with this standard varies according to the communication protocol used (RS-232, Ethernet, GPIB). After the data is received, it is stored in a line of a CSV file.

Since two devices were used for the measurements (a multimeter, for temperature measurement, and a battery tester, for the remaining characteristics), two files were created. The file corresponding to the data from the battery tester characterizes the process made, mainly the operation made (discharge or charge), the current used in the operation (in A), the nominal capacity of the battery used (in mAh) and the values retrieved from the battery tester (voltage, current, capacity) with a timestamp created during the execution of the script. In parallel to the battery tester's measurements, the multimeter performs the measurement of the temperature

at the surface of the battery and stores it in a second file, used for the storage of the type of sensor used for the measurement (RTD or NTC) and the values obtained in the measurements. The code for this section is present on appendix A

At first, these two files were supposed to be one. However, during the appending of the timestamp and consequent writing into the battery tester file, sometimes it resulted in two consecutive readings having the same timestamp. Additionally, when attempting to do the same with the temperature value, this error escalated significantly, resulting in more than 2 readings with the same timestamp, thus corrupting the values sent from the device. Both of these errors existed due to the lack of synchronicity, since each one of the measurement devices have different times regarding the reception, processing and further response to the instruction sent. This variation of instruction processing time, alongside the processes happening on the script (the appending of a value to a sample and its storage on a file) and the existence of a internal buffer (for the case of the battery tester), result in the delayed processing of the most recent samples, resulting on the occasional acquisition of a sample that contain more than one reading.

For this reason, the temperature values are separated from the tester values and any one of those values that had the same timestamp was later on eliminated. While this elimination resulted in the loss of some data, it was not a significant number (the number of samples in each file ranges from 50000 to 150000, depending on the capacities and chemistries, with only 8 to 12 samples being deemed as corrupted and therefore discarded from the dataset). In order to place all of the values in one file for better file organization, the samples from the temperature registration file were copied to the battery tester file, resulting in a file that has the structure of Figure 3.2.

Capacity: 2.05 Ah				
Discharging at 1.25A				
Voltage (V)	Current (A)	Capacity (Ah)	Timestamp (s)	Temperature (ºC)
+2.940166E+00	-1.122768E+00	+0.000000E+00	0.3517117500305176	23.1873418
+3.589361E+00	-1.122629E+00	-3.152912E-05	0.4312620162963867	23.193477
+3.589103E+00	-1.122630E+00	-6.293156E-05	0.5678703784942627	23.2046927
+3.588865E+00	-1.122603E+00	-9.445836E-05	0.6622753143310547	23.2117528
+3.588655E+00	-1.122558E+00	-1.259530E-04	0.741497278213501	23.2179564
+3.588443E+00	-1.122527E+00	-1.574777E-04	0.8879818916320801	23.2292215

Figure 3.2: Data Structure After Merging Multimeter and Battery Tester Files

Through the creation of the dataset that is going to be used by the decision system, there are some values that are expected. During the discharge process, the last voltage value has to be close of equal to the cut-off voltage, specified by the

manufacturer in the battery's datasheet. One good rule of thumb for the chemistries used on this dataset is that, for the case of lithium-based chemistries (Li-ion and LiPo), the voltage interval is situated between 3.8V and 4.2V, while for the case of nickel-based chemistries (Ni-Cd and NiMH), this interval is situated between 1V and 1.4V (since 3 cells are being used in series, this interval becomes located between 3V and 4.2V). This data, alongside the values regarding the sensing temperature of each battery are represented on figure 3.3.

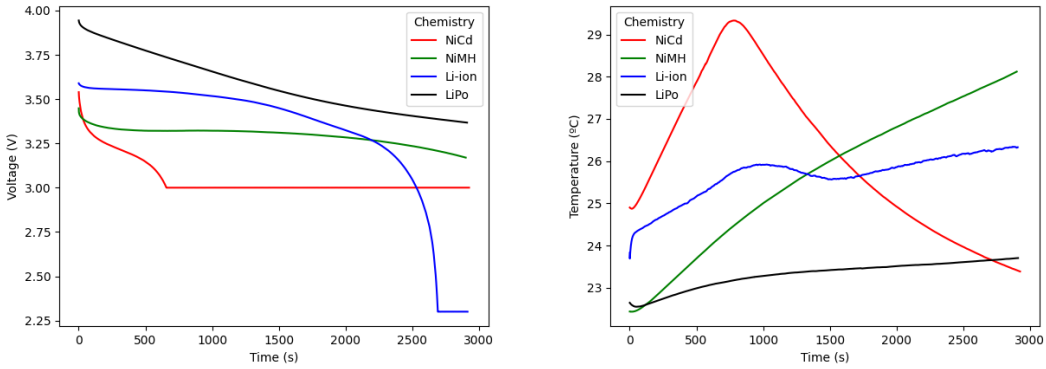

(a) Variation of voltage during discharge

(b) Variation of temperature during discharge

Figure 3.3: Analysis of measured data

In figure 3.3a, it is observeable that LiPo, NiMH and Ni-Cd batteries have terminal voltage values that are close to each other (between 3 and 3.5V), while the Li-ion battery has a smaller cut-off voltage close to 2.25V. Despite this discrepancy, it can be assumed that the discharge process is performed correctly [1].

3.4 The Decision Support System

The decision support system is developed with the purpose of, given a set of characteristics for a certain project, select the most optimal battery chemistry. With the input parameters converted to the algorithm value, they are inserted into the K-Nearest Neighbours (KNN) in order to check the distance to each one of the neighbors. KNN was chosen due to it requires very few configurations to operate (only changing the number of neighbours to be found). The implementation of the algorithm used by our decision support system is the one present in scikit-learn[80] library. The code is available in Annex B

As mentioned in the start of chapter 2, batteries have a large spectrum of characteristics. So, for this project, the quantity of the characteristics was reduced

[1] The process is considered correct when the discharge process happens in two phases: one where current is constant (and the voltage reaches the value configured), and another where voltage is constant (and the current drops up to the threshold defined in the configuration)

in order to consider the ones that have the greatest impact in the context of this work. Koniak and Czerepicki [81] defines the most essential specifications as being weight, volume, environmental temperature, output current and quantity of charging cycles), while Wendt [82] defines them as being energy and power density, the existence of the "memory effect", quantity of charging cycles and durability. From these attributes, the ones that are going to be selected for the algorithm are interval of environmental temperature (or temperature felt by the user, depending on the scenario), capacity, weight and sustainability, since they represent the battery's behavior regarding environmental or energetic hindrances. Regarding the parameter of sustainability, it is going to be defined as a value between 0 and 1 and, due to the lack of information between the comparison of the different chemistries, these values are arbitrary and attributed based on the information provided in chapter 2.

The sequence of operations that the script is going to perform are as follows:

- Characterization of the scenario - The user supplies the program with several parameters. These are: the current to be supplied, the estimated time of operation, and expected interval of temperature (either operating or sensed).
- Conversion of the inputs to algorithm variables - In this step, the values supplied by the user in the previous step will be converted to variables used for the training of the algorithm (this is the case of the capacity, calculated according to equation 2.2). This conversion also includes the normalization of the values to, when possible, values that are above the minimum and maximum values of each one of the parameters used in the training of the algorithm.
- Battery Selection - With the input parameters converted to the algorithm values, they are inserted into the KNN in order to check the distance to each one of the neighbors. There are 2 models that have been trained with two different sets, one is for static applications (for its use as an uninterruptible power supply or supplying static devices such as dishwashers) and the other is for more mobile applications (to be used in devices such as smartphones and medical devices). After the algorithm calculates the distance between the inputs and each one of the neighbors, it checks if each one of the batteries' values is located within the specifications (for instance, in a case where the temperature interval of the project is between 10ºC and 40ºC, this processing excludes every battery whose temperature interval is not located within 10ºC and 40ºC).
- Presentation of the most optimal choice - After the previous processing is made, the filtered batteries are presented on a table, ordered by the distance.

Usually, in these types of algorithms, the training set is made of large quantities of data from different scenarios. For the development of this project, and with the

assistance of the data that was previously obtained, the values that are obtained will be either maximum and minimal (for the case of temperature) or derived from manufacturer information (for the case of nominal capacity and weight).

For the training, the information is derived from 2 batteries from 4 different chemistries (Ni-Cd, NiMH, Li-ion and LiPo). This information is classified based on the values in table 3.1. Because these values have different dimensions (capacity interval is significantly smaller and has smaller values when compared to the rest), they are going to be normalized. The purpose of normalization is so that all values have the same scalability and interval dimension (between 0 and 1).

The values that are present in this table are sorted by cell column and position inside the cell itself and later inserted in the KNN algorithm for its training process. As explained previously, this algorithm is different from other alternatives since it stores the entirety of the data instead of storing only the patterns that differentiate each battery.

Chemistry	NiCd	NiMH	Li-ion	LiPo
Sense Temperature interval (ºC)	23-29	22-30	24-34	21-27
	23-28	24-30	23-29	24-29
Nominal Capacity (Ah)	0.7	1.3	1.3	1.35
	1.5	1.9	2.05	2
Weight (g)	23	23	27	29
	126	27	45	40
Sustainability (0-1)	0	1	0.5	0.5
	0	1	0.5	0.5

Table 3.1: Characteristics of batteries in analysis

Because these values have different dimensions (capacity interval is significantly smaller and has smaller values when compared to the rest), they are going to be normalized. The purpose of normalization is so that all values have the same scalability and interval dimension (between 0 and 1).

After the algorithm has been trained with the normalized values, it is ready to be run and give responses based on the user's input. For this purpose, the user will not give the specific parameters of the algorithm. Instead, what is being transmitted are parts of the parameters. The parameters used in the algorithm's training can be either calculated (capacity) or measured (voltage, current, weight and temperature). So, the process that occurs from the reception of the values given by the user to the classification algorithm is performed with the structure shown earlier in this chapter, followed by the calculation of the capacity using equation 2.2, previously showed in chapter 2.1.

3.5 Experimental Setup Limitations

As stated in the previous sections, the project developed is going to be settled on the KNN algorithm. This algorithm calculates the distance between the neighbor created by the user and each one of the neighbors present in the trained model. For this project, the model has been trained according to data from previous sections.

Although it uses the KNN as its selection method, there are several limitations that were implemented to assure a higher viability of results. Since the model used in the algorithm does not include the characteristics of batteries of all chemistries and manufacturers, the limitations implemented were designed in function of the values used in the model training. This affects several battery specifications, such as electrical specifications (battery capacity capped at 2.1Ah) and thermal ones (upper temperature limit capped at 65ºC (static scenarios) and 33.53ºC (wearable scenarios) and lower temperature limit capped at -20ºC (static scenarios) and 21.14ºC (wearable scenarios)).

In this section, the model is going to be evaluated by taking into consideration the fact that the battery selected is going to be supplying a computer mouse based on a reference design by Texas Instruments [83]. Its electrical circuit is comprised of the following components: an LED sensor (HLMP-ED80), an optical mouse sensor (ADNS-3040), a microcontroller (MSP430F1222) for processing signals that come from the external buttons and devices, a module for transmitting the information via Bluetooth to a local computer (TRF7950) (see full architecture in appendix C.

When it comes to the total consumption of this circuit, it is estimated that the total current value required for its correct operation is 90mA. This value was calculated without the current consumption of the Bluetooth module, since information about its specifications was not found. Due to a lack of information regarding autonomy tests or expected operating temperature interval, it is going to be considered in this section that the mouse is going to operate at room temperature (25ºC) for one day (24h), and its type of operation is static (since it does not come into close contact with the human skin. Table 3.2 shows the batteries that are most suited for use in this prototype, ordered by the distance between the user's specifications and each one of the training values used.

Identification	Distance	Tmin (ºC)	Tmax (ºC)	Capacity (Ah)	Weight (g)	Sustainability
Specs	**0**	**25**	**25**	**2.16**	**0**	**1**
NiMH 1.9Ah	3.93	0	50	1.9	81	1
LiPo 1.35Ah	5.14	-10	55	1.35	29	0.5
LiPo 2Ah	5.61	-20	60	2	40	0.5
Li-ion 2.05Ah	5.62	-20	60	2.05	45	0.5
Li-ion 1.3Ah	5.99	-20	60	1.3	27	0.5
NiMH 1.3Ah	6.25	-20	65	1.3	69	1
NiCd 1.5Ah	7.01	-20	55	1.5	126	0
NiCd 0.7Ah	7.36	-20	60	0.7	69	0

Table 3.2: Battery analysis based on prototype requirements

Chapter 4

Results and Discussion

For this chapter, several use cases are going to be described to implement and check the algorithm's behavior in real-life situations. These use cases will analyze the characteristics of some battery parameters in specific scenarios, such as the case of temperature (in a domestic use case) and battery mass (low mass particularly).

4.1 Use Cases

4.1.1 Domestic Use Case

Conposting[84] is a project developed by Fraunhofer Portugal AICOS in partnership with LiPor whose purpose consists in the analysis of homemade composting data (temperature and humidity inside the composting device) and transmission of this same data via a LoRa transducer, equipped with an antenna. This data is measured 2 times per day.

For this project, the composting device was made with an electrical circuit developed at Fraunhofer Portugal AICOS. The circuit consists of a power supply system (which includes a battery, a fuel gauge connected to the battery for capacity monitorization, and a DC/DC buck converter to convert the current from the battery to a lower value that is supported by the remaining components), a central processing unit (made of a microcontroller, connected to a LoRa module and antennae), a sensing system (comprising of a sensor for temperature and humidity reading), and a LED for checking the status of the sensor.

The requirements of each one of the components used in the development of the project is indicated in table 4.1.

Component	Current (μA)
Microcontroller + Transceiver	124700 (Tx); 16700 (Rx)
Sensor	150 (humidity reading); 90 (temperature reading)
Fuel Gauge	35
LED	5000
DC/DC	200000 (for supplying the system)

Table 4.1: Electrical requirements for the project operation

The estimated current consumption of this project (from the measurement of temperature and humidity to the sending of the data to the backend) is the sum of all the electric components from line 1 to line 4 of the previous table, making a total of 146,675 mA (since it does not give information regarding the time that each component takes in performing its tasks, it is going to be considered as being 1 second. With this consideration, the capacity required to run this circuit one time is $146.675 * 1/3600 = 0.0407mAh$). This value is what the system consumes per data acquisition. Considering that the system acquires values of humidity and temperature 2 times per day over a time period of 30 days, the capacity value that is required is 2.4Ah. Consolidating this information alongside the operating temperature of the battery (between -5ºC and 85ºC, according to [84]) and considering this battery application as being static, or not in direct contact with the human skin, the trained algorithm returns the structure defined in table 4.2.

Identification	Distance	Tmin (ºC)	Tmax (ºC)	Capacity (Ah)	Weight (g)	Sustainability
Specs	**0**	**-5**	**65**	**2.4**	**0**	**1**
NiMH 1.3Ah	2.82	-20	65	1.3	69	1

Table 4.2: Battery analysis based on Conposting project [84] requirements

According to the algorithm's choice presented in table 4.2, the battery that appears as being the most optimal for the given specifications is the one identified as "NiMH 1.3Ah". One thing to consider is that, since the upper temperature value is larger than that of the highest upper temperature in the trained model, this value is going to be limited in the algorithm (that is why it appears the upper temperature as being 65ºC instead of 85ºC).

This battery chemistry has the best score regarding its environmental impact, and it also contributed to the selection of this battery. One of the downfalls of this battery is that its capacity is significantly lower than is required by the project. Another of the batteries with a higher capacity could have been chosen ("NiMH

1.9Ah", "LiPo 2Ah" or "Li-ion 2.05Ah"). However, these were not selected because their temperature interval did not fit in the one specified by the user.

4.1.2 Agriculture Use Case

Lora4UProbes [85] is a project developed at Fraunhofer Portugal AICOS alongside Aquagri. Its purpose resides in the development of a datalogger that is buried underground and performs probe measurements of soil conditions (temperature, salinity and volumetric water content) and sends this information to a remote server. The measurements are performed every 15 minutes and transmission of the measurements every hour (60 minutes).

For this case, the device designed is made of a probe that measures the soil conditions mentioned in the previous paragraph, followed by a LoRa module (equipped with an external antenna) for transmission of the measurements to a remote server.

Table 4.3 presents the electrical characteristics of each one of these components. These values were tested using Nordic's Power Profile Kit II (both the current consumption and the time length for measuring or transmitting the measurements).

Component	Current (mA)	Time (ms)
Probe	9.87 (Volumetric water content measurement)	891.8
	7.53 (Salinity measurement)	1897.0
	4.13 (Temperature measurement)	805.7
LoRa module	29.35 (@ 14 dBm)	92.4
IoT prototype	70.33	16780

Table 4.3: Electrical requirements for Lora4UProbes [85]

With this data, in order to perform the three measurements (Volumetric water content, salinity and temperature), the capacity that is going to be required for the three operations sums up to a value of approximately 32.19 mAh per day. The main purpose of this project was to use a battery that could perform these measurements + transmission for a time period of 1 year. Additionally, the battery is meant to be operated at room temperature (approximately 25ºC). For the reason of better analysis of this case's application to the algorithm, the autonomy of the battery is going to be considered as being 2 months instead of 1 year. Given the product specifications and the time of operation that the battery is going to be working on, as well as this application having a static type of operation, the capacity necessary for the operation of the battery is going to be 1.8Ah. The selection of the battery given the specifications for this project is shown in table 4.4

For this project's specifications, the battery that is seen as the most adequate is labeled "NiMH 1.9Ah". This particular case does not have a temperature interval but instead has one temperature value (25ºC). For this reason, since the batteries

Identification	Distance	Tmin (ºC)	Tmax (ºC)	Capacity (Ah)	Weight (g)	Sustainability
Specs	**0**	**25**	**25**	**1.8**	**0**	**1**
NiMH 1.9Ah	3.81	0	50	1.9	81	1
LiPo 1.35Ah	4.88	-10	55	1.35	29	0.5
LiPo 2Ah	5.64	-20	60	2	40	0.5
Li-ion 2.05Ah	5.72	-20	60	2.05	45	0.5
Li-ion 1.3Ah	5.73	-20	60	1.3	27	0.5
NiMH 1.3Ah	5.98	-20	65	1.3	69	1
NiCd 1.5Ah	6.74	-20	55	1.5	126	0
NiCd 0.7Ah	7.10	-20	60	0.7	69	0

Table 4.4: Battery analysis based on Lora4UProbes project [85] requirements

used for the algorithm training have a large interval of temperature, regarding the thermal specifications, every one of the batteries is fit for this project.

However, the selection of the "NiMH 1.9Ah" battery can prove fruitful for this project. This is because the capacity value is approximate to the one introduced by the user (the battery has 1.9Ah, and this case requires 1.8Ah), resulting in a good approximation. While there are other batteries that have higher capacity ("LiPo 2Ah" and "Li-ion 2.05Ah"), the "NiMH 1.9Ah" has a lower impact on the environment, thus becoming an optimal choice for projects where the leakage of chemicals from the cells can result in harmful effects to the environment.

4.1.3 Medical Use Case

Wearable applications are starting to become present in the medical sector. Portable medical devices can be used by patients in their everyday lives for monitoring vital signals, such as heart rate. These signals, often included with a central processing unit, can perform real-time processing of this information, followed by its dispatch to the attending physician for further analysis.

The prototype developed in this article by Martin et al [86] is a wearable Electrocardiogram (ECG) monitor. An ECG's mode of operation starts by reading cardiac signals transmitted through the human central nervous system (as electrical signals of reduced amplitude) with the assistance of electrodes. These electrodes capture the electrical signal and after frequency filtering and amplification are sent to a machine in order to be converted into a digital signal, which is often observed as a graphical representation.

The prototype proposed by the authors consists in the use of a Del Mar PWA Amplifier, for amplifying the analog signal that comes from the surface of the skin, and a TMS320C5410-100 processor board, for performing digital signal processing and sending its information to a local or remote user.

The average consumption of this prototype is about 0.150 A, and it is expected to operate for 10 hours. The authors do not give information regarding the operating

temperature of this prototype, but since this prototype is meant to be used as a wearable device, the temperature that the battery can reach must not be too high, since it can result in the discomfort of using the device in question. According to a study made by Hepokoski et al [87], subjects started to sense discomfort when using a wearable device when the device's surface temperatures reached 34ºC. For this reason, and taking this study into consideration, the temperature interval of ECG device is limited to the interval between 25ºC (which is the room temperature, and the starting point of the study of Hepokoski et al [87]) and 34ºC.

Table 4.5 shows the proximity of batteries that are most optimal for the requirements given by the authors.

Identification	Distance	Tmin (ºC)	Tmax (ºC)	Capacity (Ah)	Weight (g)	Sustainability
Specs	**0**	**25**	**33.53**	**1.5**	**0**	**1**
Li-ion 1.3Ah	1.36	23.71	33.53	1.3	27	0.5

Table 4.5: Battery analysis based on Martin et al [88] prototype requirements

From table 4.5, the algorithm selected the "Li-ion 1.3Ah" battery as being the one that fits most into the project's specifications. One of the observation parameters for this case is that of the battery weight, and the battery selected is the lightest of the entire dataset (27g), and its capacity is close to the specified by the user, although it is smaller (1.3Ah of the battery VS 1.5Ah specified by the user).

However, using this chemistry in a wearable device such as the ECG can result in leakage of internal reagents which, when in contact with human skin or organs (if the ECG is inside the person) can have harmful consequences.

Chapter 5

Conclusion and Future Work

The use of batteries has contributed to the portability of devices that once were fixed. Furthermore, this canister of chemical materials has evolved to being able to withstand large amounts of energy stored inside it. However, the diversity of battery chemistries and sizes often leads the end consumer to select one that is cheap, light and has a high capacity value. The solution presented in this report aims to observe the chemistries available on the market, mainly the 4 that are most used in projects related to IoT (Li-ion, LiPo, Ni-Cd and NiMH) and select the most adequate option for projects based on its electrical specifications.

The first step in the project development resided in the acquisition of data regarding the battery's performance behavior. For this step, two devices and a set of batteries were used for the generation of these sets of values. While the values obtained were the ones that were expected from a theoretical point of view, its writing in a external file proved to have an extra step due to the devices' different sampling time.

Following the acquisition of data, they were used for the training of the KNN model. However, the values that were used had ranges with different dimensions (as is observed for the case of temperature intervals and capacity values in table 3.1). As a consequence, the KNN model ended up attributing a different weight for each one of the parameters. The normalization of each one of these values, as well as the inputs provided by the user, resulted in an improved scalability of the dataset, resulting in an equal distribution of the weight from the model's point of view.

However, while using KNN was proven advantageous due to its simplicity and unsupervised alternative, it does not work as intended in scenarios where two batteries have very similar characteristics. One example of this is that, with batteries with the same temperature interval and weight but with different capacities, the model chooses the battery with the lowest capacity (having the smallest distance between the neighbors and the user's specs). To improve this algorithm and correct this setback, an optimization algorithm could be implemented in order to better optimize results and provide a more reliable outcome.

In addition to this implementation, there are other extra features that could be implemented alongside this battery classification solution. These extras consist in the calculation of the battery's SoC and SoH through the values obtained during the step of data acquisition in this project. These parameters can become relevant in the situation where a battery has been used for a long time, where it is checked if replacement is necessary (for the case of SoH), or if the battery is properly charged to its maximum capacity (for the case of SoC).

References

[1] Y. Zhao, O. Pohl, A. I. Bhatt, G. E. Collis, P. J. Mahon, T. Rüther, and A. F. Hollenkamp, "A review on battery market trends, second-life reuse, and recycling," *Sustainable Chemistry*, vol. 2, no. 1, p. 167–205, 2021. [Cited on page 2]

[2] C. Hendricks, N. Williard, S. Mathew, and M. Pecht, "A failure modes, mechanisms, and effects analysis (fmmea) of lithium-ion batteries," *Journal of Power Sources*, vol. 297, pp. 113–120, 2015. [Cited on pages 2 and 13]

[3] B. University, "Will secondary batteries replace primaries?." Available: `https://batteryuniversity.com/article/will-secondary-batteries-replace-primaries`, Mar 2022. Accessed on: May, 2023. [Online]. [Cited on page 5]

[4] C. Catchpole, D. Pearson, A. Siefker, and E. Gibbemeyer, "What's better, primary or secondary batteries? - university of dayton." Available: `https://ecommons.udayton.edu/cgi/viewcontent.cgi?article=2649&amp;context=stander_posters`. Accessed on: March, 2023. [Online]. [Cited on page 5]

[5] J. Zhang, L. Zhang, F. Sun, and Z. Wang, "An overview on thermal safety issues of lithium-ion batteries for electric vehicle application," *IEEE Access*, vol. 6, pp. 23848–23863, 2018. [Cited on pages vii and 6]

[6] J. W. Fergus, "Ceramic and polymeric solid electrolytes for lithium-ion batteries," *Journal of Power Sources*, vol. 195, no. 15, pp. 4554–4569, 2010. [Cited on page 6]

[7] I. Silicon Laboratories, "Selecting the optimal battery for your embedded application." Available: `https://www.silabs.com/documents/public/white-papers/Selecting-the-Optimal-Battery-WP.pdf`. Accessed on: January, 2023. [Online]. [Cited on page 7]

[8] H. Abdi, B. Mohammadi-ivatloo, S. Javadi, A. R. Khodaei, and E. Dehnavi, "Chapter 7 - energy storage systems," in *Distributed Generation Systems* (G. Gharehpetian and S. M. Mousavi Agah, eds.), pp. 333–368, Butterworth-Heinemann, 2017. [Cited on page 7]

[9] E. Seran, M. Godefroy, E. Pili, N. Michielsen, and S. Bondiguel, "What we can learn from measurements of air electric conductivity in 222rn-rich atmosphere," *Earth and Space Science*, vol. 4, no. 2, p. 91–106, 2017. [Cited on page 7]

[10] A. Aktaş and Y. Kirçiçek, "Chapter 5 - solar hybrid systems and energy storage systems," in *Solar Hybrid Systems* (A. Aktaş and Y. Kirçiçek, eds.), pp. 87–125, Academic Press, 2021. [Cited on pages 8 and 14]

[11] M. Beaudin, H. Zareipour, A. Schellenberg, and W. Rosehart, "Chapter 1 - energy storage for mitigating the variability of renewable electricity sources," in *Energy Storage for Smart Grids* (P. Du and N. Lu, eds.), pp. 1–33, Boston: Academic Press, 2015. [Cited on page 8]

[12] M. Fetcenko, J. Koch, and M. Zelinsky, "6 - nickel–metal hydride and nickel–zinc batteries for hybrid electric vehicles and battery electric vehicles," in *Advances in Battery Technologies for Electric Vehicles* (B. Scrosati, J. Garche, and W. Tillmetz, eds.), Woodhead Publishing Series in Energy, pp. 103–126, Woodhead Publishing, 2015. [Cited on page 8]

[13] Y. Ding, Z. P. Cano, A. Yu, J. Lu, and Z. Chen, "Automotive li-ion batteries: Current status and future perspectives," *Electrochemical Energy Reviews*, vol. 2, no. 1, p. 1–28, 2019. [Cited on page 8]

[14] P. Ruetschi and R. T. Angstadt, "Self-discharge reactions in lead-acid batteries," *Journal of The Electrochemical Society*, vol. 105, no. 10, p. 555, 1958. [Cited on page 8]

[15] S. S. Solutions. Available: urlhttps://www.sbsbattery.com/PDFs/$SBS_W P_1 01_B attComp-WithRefs.pdf. Accessedon : February, 2023.[Online]. [Citedonpage9]$

[16] B. University, "Bu-1006: Cost of mobile and renewable power." Available: `https://batteryuniversity.com/article/bu-1006-cost-of-mobile-and-renewable-power`, 2022. Accessed on: June, 2023. [Online]. [Cited on pages 9 and 11]

[17] Q. Government, "Impacts of acid sulfate soils." Available: `https://www.qld.gov.au/environment/land/management/soil/acid-sulfate/impacts`, 2019. Accessed on: February, 2023. [Online]. [Cited on pages 9 and 18]

[18] T. C. on Environmental Quality, "Air pollution from lead." Available: `https://www.tceq.texas.gov/airquality/sip/criteria-pollutants/sip-lead`, 2023. Accessed on: February, 2023. [Online]. [Cited on page 9]

[19] D. Vutetakis, "Applications – transportation | aviation: Battery," in *Encyclopedia of Electrochemical Power Sources* (J. Garche, ed.), pp. 174–185, Amsterdam: Elsevier, 2009. [Cited on page 10]

[20] K. Khan, M. Hossain, A. K. M. Obaydullah, and M. Wadud, "Pkl electrochemical cell and the peukert's law," *International Journal Of Advance Research And Innovative Ideas In Education*, vol. 4, pp. 4219–4227, 04 2018. [Cited on pages 10, 11, and 12]

[21] D. Hahn, "The best uses for nickel cadmium (ni-cd) batteries," Jan 2021. [Cited on page 10]

[22] Panasonic, "The memory effect in batteries: What it is and how to prevent it." Available: `https://www.panasonic-eneloop.eu/en/news/memory-effect-batteries-what-it-and-how-prevent-it`. Accessed on: February, 2023. [Online]. [Cited on page 10]

[23] D. D. Agwu, F. Opara, N. Chukwuchekwa, D. Dike, and L. Uzoechi, "Review of comparative battery energy storage systems (bess) for energy storage applications in tropical enviroments," *3rd International Conference on Electro-Technology for National Development*, 09 2018. [Cited on pages vii, 10, 12, and 15]

[24] B. Hariprakash, A. Shukla, and S. Venugoplan, "Secondary batteries – nickel systems | nickel–metal hydride: Overview," in *Encyclopedia of Electrochemical Power Sources* (J. Garche, ed.), pp. 494–501, Amsterdam: Elsevier, 2009. [Cited on page 11]

[25] S. T. Revankar, "Chapter six - chemical energy storage," in *Storage and Hybridization of Nuclear Energy* (H. Bindra and S. Revankar, eds.), pp. 177–227, Academic Press, 2019. [Cited on page 11]

[26] R. Amui and J. Nkurunziza, *Commodities at a glance*. United Nations, 10 2020. [Cited on pages 11, 12, 13, and 16]

[27] H. Zhang, Y. Yang, D. Ren, L. Wang, and X. He, "Graphite as anode materials: Fundamental mechanism, recent progress and advances," *Energy Storage Materials*, vol. 36, pp. 147–170, 2021. [Cited on pages 11 and 16]

[28] L. Power, "Protection circuit module - litechpower.com." Available: `https://www.litechpower.com/htmledit/uploadfiles//20180322200327014.pdf`. Accessed on: April, 2023. [Online]. [Cited on pages vii and 13]

[29] A. Murray, "Cobalt mining: The dark side of the renewable energy transition." Available: `https://earth.org/cobalt-mining/`, Sep 2022. Accessed on: June, 2023. [Online]. [Cited on page 12]

[30] L. Mucha, T. C. Frankel, and K. D. Sadof, "The hidden costs of cobalt mining," Oct 2021. [Cited on page 13]

[31] M. Posner, "To meet global cobalt demand, companies must reform mining practices in the congo," Feb 2023. [Cited on page 13]

[32] A. Dobie, "Recalling the samsung galaxy note 7, five years later." Available: `https://www.androidcentral.com/recalling-galaxy-note-7-five-years`, Aug 2021. Accessed on: June, 2023. [Online]. [Cited on page 13]

[33] J. Rogan, "Are solid-state batteries the solution to liquid electrolytes?." Available: `https://www.vennershipley.co.uk/insights-events/are-solid-state-batteries-the-solution-to-liquid-electrolytes/`, 2022. Accessed on: June, 2023. [Online]. [Cited on page 14]

[34] National Research Council (US) Chemical Sciences Roundtable, *Critical materials in large-scale battery applications*. Washington, D.C., DC: National Academies Press, 2012. [Cited on page 14]

[35] H. Chen, Y. Xu, C. Liu, F. He, and S. Hu, "32 - storing energy in china—an overview," in *Storing Energy (Second Edition)* (T. M. Letcher, ed.), pp. 771–791, Elsevier, second edition ed., 2022. [Cited on pages 15 and 17]

[36] J. Ma, F. Li, Z. Wei, Y. Feng, A. Manthiram, and L. Mai, "Sodium-based batteries: From critical materials to battery systems," *Journal of Materials Chemistry A*, vol. 7, 03 2019. [Cited on pages vii and 15]

[37] A. M. Skundin, T. L. Kulova, and A. B. Yaroslavtsev, "Sodium-ion batteries (a review)," *Russian Journal of Electrochemistry*, vol. 54, no. 2, p. 113–152, 2018. [Cited on page 16]

[38] J. Peters, A. Peña Cruz, and M. Weil, "Exploring the economic potential of sodium-ion batteries," *Batteries*, vol. 5, no. 1, p. 10, 2019. [Cited on page 16]

[39] N. Yabuuchi, K. Kubota, M. Dahbi, and S. Komaba, "Research development on sodium-ion batteries," *Chemical Reviews*, vol. 114, p. 11636–11682, Nov 2014. [Cited on page 16]

[40] Z. Li, Y. Zhang, J. Zhang, Y. Cao, J. Chen, H. Liu, and Y. Wang, "Sodium-ion battery with a wide operation-temperature range from -70 to 100°c," *Angewandte Chemie International Edition*, vol. 61, Jan 2022. [Cited on page 16]

[41] Solaradvisor, "Lithium-ion vs sodium-ion batteries: Which is the better one?," Feb 2022. [Cited on pages 16 and 17]

[42] A. Parasuraman, T. M. Lim, C. Menictas, and M. Skyllas-Kazacos, "Review of material research and development for vanadium redox flow battery applications," *Electrochimica Acta*, vol. 101, pp. 27–40, 2013. [Cited on page 17]

[43] A. Arabkoohsar, "Chapter one - classification of energy storage systems," in *Mechanical Energy Storage Technologies* (A. Arabkoohsar, ed.), pp. 1–12, Academic Press, 2021. [Cited on page 17]

[44] J. Ferrari, "Chapter 3 - energy storage and conversion," in *Electric Utility Resource Planning* (J. Ferrari, ed.), pp. 73–107, Elsevier, 2021. [Cited on pages vii, 17, and 18]

[45] C. Doetsch and A. Pohlig, "13 - the use of flow batteries in storing electricity for national grids," in *Future Energy (Third Edition)* (T. M. Letcher, ed.), pp. 263–277, Elsevier, third edition ed., 2020. [Cited on page 18]

[46] S. K. Pradhan and B. Chakraborty, "Battery management strategies: An essential review for battery state of health monitoring techniques," *Journal of Energy Storage*, vol. 51, p. 104427, 2022. [Cited on pages 19, 20, 22, and 23]

[47] ANSMANN, *2632686.pdf*, 2018. [Cited on pages vii and 20]

[48] H. S. Magar, R. Y. Hassan, and A. Mulchandani, "Electrochemical impedance spectroscopy (eis): Principles, construction, and biosensing applications," *Sensors*, vol. 21, Oct 2021. [Cited on page 21]

[49] L. A. Middlemiss, A. J. Rennie, R. Sayers, and A. R. West, "Characterisation of batteries by electrochemical impedance spectroscopy," *Energy Reports*, vol. 6, pp. 232–241, 2020. 4th Annual CDT Conference in Energy Storage & Its Applications. [Cited on pages vii, 21, and 22]

[50] A. Viana, F. Pereira, and M. Alves, "Circuitos de corrente alternada monofásica." 2016. [Cited on page 21]

[51] J. Kennedy and R. Eberhart, "Particle swarm optimization," in *Proceedings of ICNN'95 - International Conference on Neural Networks*, vol. 4, pp. 1942–1948 vol.4, 1995. [Cited on page 22]

[52] Y. Chen, D. Huang, Q. Zhu, W. Liu, C. Liu, and N. Xiong, "A new state of charge estimation algorithm for lithium-ion batteries based on the fractional unscented kalman filter," *Energies*, vol. 10, p. 1313, 09 2017. [Cited on pages vii and 23]

[53] E. Chemali, P. J. Kollmeyer, M. Preindl, and A. Emadi, "State-of-charge estimation of li-ion batteries using deep neural networks: A machine learning approach," *Journal of Power Sources*, vol. 400, pp. 242–255, 2018. [Cited on page 24]

[54] A. Becker, "Kalman filter tutorial." Available: `https://www.kalmanfilter.net/`. Accessed on: February, 2023. [Cited on pages vii and 25]

[55] P. Spagnol, S. Rossi, and S. M. Savaresi, "Kalman filter soc estimation for li-ion batteries," in *2011 IEEE International Conference on Control Applications (CCA)*, pp. 587–592, Sep. 2011. [Cited on pages vii, 25, 26, and 27]

[56] X. Zhang, *Structural Risk Minimization*, pp. 929–930. Boston, MA: Springer US, 2010. [Cited on page 27]

[57] D. Bzdok, M. Krzywinski, and N. Altman, "Machine learning: Supervised methods, SVM and kNN," *Nature Methods*, pp. 1–6, Jan. 2018. [Cited on pages vii and 28]

[58] Editorial, "Pros and cons of support vector machine (svm)," Sep 2022. [Cited on page 28]

[59] Z. Chen, M. Sun, X. Shu, R. Xiao, and J. Shen, "Online state of health estimation for lithium-ion batteries based on support vector machine," *Applied Sciences*, vol. 8, no. 6, p. 925, 2018. [Cited on page 28]

[60] C. Hu, G. Jain, P. Zhang, C. Schmidt, P. Gomadam, and T. Gorka, "Data-driven method based on particle swarm optimization and k-nearest neighbor regression for estimating capacity of lithium-ion battery," *Applied Energy*, vol. 129, p. 49–55, 2014. [Cited on pages vii, 29, and 30]

[61] E. Keogh, *Instance-Based Learning*, pp. 549–550. Boston, MA: Springer US, 2010. [Cited on pages 28 and 29]

[62] K. Taunk, S. De, S. Verma, and A. Swetapadma, "A brief review of nearest neighbor algorithm for learning and classification," in *2019 International Conference on Intelligent Computing and Control Systems (ICCS)*, pp. 1255–1260, 2019. [Cited on page 29]

[63] Genesis, "Pros and cons of k-nearest neighbors," Sep 2018. [Cited on page 29]

[64] K. A. Severson, P. M. Attia, N. Jin, N. Perkins, B. Jiang, Z. Yang, M. H. Chen, M. Aykol, P. K. Herring, D. Fraggedakis, M. Z. Bazant, S. J. Harris, W. C. Chueh, and R. D. Braatz, "Data-driven prediction of battery cycle life before capacity degradation," *Nat. Energy*, vol. 4, pp. 383–391, Mar. 2019. [Cited on page 30]

[65] Z. Chen, Q. Xue, R. Xiao, Y. Liu, and J. Shen, "State of health estimation for lithium-ion batteries based on fusion of autoregressive moving average model and elman neural network," *IEEE Access*, vol. 7, pp. 102662–102678, 2019. [Cited on page 31]

[66] B. Saha and K. Goebel, "Battery data set," in *NASA Prognostics Data Repository*, 2007. [Cited on pages vii, 31, and 32]

[67] G. Ma, Y. Zhang, C. Cheng, B. Zhou, P. Hu, and Y. Yuan, "Remaining useful life prediction of lithium-ion batteries based on false nearest neighbors and a hybrid neural network," *Applied Energy*, vol. 253, p. 113626, 2019. [Cited on pages 32 and 33]

[68] S. Jo, S. Jung, and T. Roh, "Battery state-of-health estimation using machine learning and preprocessing with relative state-of-charge," *Energies*, vol. 14, p. 7206, Nov 2021. [Cited on page 33]

[69] P. Kollmeyer, "Panasonic 18650pf li-ion battery data." Available: `https://data.mendeley.com/datasets/wykht8y7tg/1`, 2018. Accessed on: April, 2023. [Online]. [Cited on pages vii and 33]

[70] R. Zhao, P. J. Kollmeyer, R. D. Lorenz, and T. M. Jahns, "A compact unified methodology via a recurrent neural network for accurate modeling of lithium-ion battery voltage and state-of-charge," in *2017 IEEE Energy Conversion Congress and Exposition (ECCE)*, pp. 5234–5241, 2017. [Cited on page 33]

[71] E. Chemali, P. J. Kollmeyer, M. Preindl, R. Ahmed, and A. Emadi, "Long short-term memory networks for accurate state-of-charge estimation of li-ion batteries," *IEEE Transactions on Industrial Electronics*, vol. 65, no. 8, pp. 6730–6739, 2018. [Cited on page 33]

[72] U. of Maryland, "Battery data," in *Battery Data*. [Cited on page 33]

[73] F. Zheng, Y. Xing, J. Jiang, B. Sun, J. Kim, and M. Pecht, "Influence of different open circuit voltage tests on state of charge online estimation for lithium-ion batteries," *Applied Energy*, vol. 183, pp. 513–525, 2016. [Cited on page 34]

[74] Y. Wang, C. Liu, R. Pan, and Z. Chen, "Experimental data of lithium-ion battery and ultracapacitor under DST and UDDS profiles at room temperature," *Data in Brief*, vol. 12, pp. 161–163, 2017. [Cited on pages vii, 34, and 35]

[75] S. Li, H. He, and J. Li, "Big data driven lithium-ion battery modeling method based on sdae-elm algorithm and data pre-processing technology," *Applied Energy*, vol. 242, pp. 1259–1273, 2019. [Cited on page 34]

[76] Keithley, "Model 2281s-20-6 precision dc power supply and battery simulator." Available: `https://download.tek.com/manual/077114601_2281_Ref_Mar_2019.pdf`, 2019. Accessed on: April, 2023. [Online]. [Cited on page 38]

[77] O. Engineering, "Ntc thermistors vs. resistance temperature detectors (rtds)." Available: `https://www.omega.com/en-us/resources/rtd-vs-thermistors`. Accessed on: July, 2023. [Cited on page 38]

[78] I. Foundation, "Scpi." Available: https://www.ivifoundation.org/scpi/. Accessed on: April, 2023. [Online]. [Cited on page 39]

[79] PyVISA, "Pyvisa: Control your instruments with python." Available: https://pyvisa.readthedocs.io/en/latest/index.html. Accessed on: April, 2023. [online]. [Cited on page 39]

[80] F. Pedregosa, G. Varoquaux, A. Gramfort, V. Michel, B. Thirion, O. Grisel, M. Blondel, P. Prettenhofer, R. Weiss, V. Dubourg, J. Vanderplas, A. Passos, D. Cournapeau, M. Brucher, M. Perrot, and E. Duchesnay, "Scikit-learn: Machine learning in Python," *Journal of Machine Learning Research*, vol. 12, pp. 2825–2830, 2011. [Cited on page 42]

[81] M. Koniak and A. Czerepicki, "Selection of the battery pack parameters for an electric vehicle based on performance requirements," *IOP Conference Series: Materials Science and Engineering*, vol. 211, p. 012005, 2017. [Cited on page 43]

[82] Z. Wendt, "5 essential factors for choosing the right battery." Available: https://www.arrow.com/en/research-and-events/articles/choosing-the-right-battery-for-your-internet-of-things-application, 2022. Accessed on: May, 2023. [Online]. [Cited on page 43]

[83] R. Wu, *Ultra-Low-Power 27-MHz Wireless Mouse Reference Design*, 2006. [Cited on pages vii, 45, and 73]

[84] A. Pereira, C. Resende, D. Correia, E. Oliveira, G. Lemos, R. Graça, and T. Rocha, "Conposting - Especificação do Sistema de Monitorização e Comunicação de Dados de Compostagem Caseira," tech. rep., Fraunhofer Center for Assistive Information and Communication Solutions – AICOS, Rua Alfredo Allen 455/461, 4200-135 Porto, PORTUGAL, Aug 2020. [Cited on pages 47 and 48]

[85] D. Sousa, R. Moutinho, C. Resende, J. Oliveira, M. Roque, R. Graça, A. Júnior, W. Júnior, and L. Carvalho, "Underground sensing probes for precision agriculture," in *International Conference on Agricultural Engineering (AgEng-LAND.TECHNIK 2022)*, pp. 625–630, EurAgEng, VDI Wissensforum, 2022. [Cited on pages 49 and 50]

[86] T. Martin, E. Jovanov, and D. Raskovic, "Issues in wearable computing for medical monitoring applications: a case study of a wearable ecg monitoring device," in *Digest of Papers. Fourth International Symposium on Wearable Computers*, pp. 43–49, 2000. [Cited on page 50]

[87] M. Hepokoski, A. Curran, T. Viola, and A. Ockfen, "Thermal acceptability limits for wearable electronic devices," in *2021 37th Semiconductor Thermal*

Measurement, Modeling & Management Symposium (SEMI-THERM), pp. 16–19, 2021. [Cited on page 51]

[88] H.-S. Song, J.-B. Jeong, B.-H. Lee, D.-H. Shin, B.-H. Kim, T.-H. Kim, and H. Heo, "Experimental study on the effects of pre-heating a battery in a low-temperature environment," in *2012 IEEE Vehicle Power and Propulsion Conference*, pp. 1198–1201, 2012. [Cited on page 51]

Appendix A

Connection file between computer and measurement devices

```
1
2  import traceback
3  import time
4  import csv
5  from BatEval_devCon import battery_charge, battery_discharge,
       device_connection, error_handler,
       multmeter_temperature_configuration
6
7
8  # Vari veis Globais
9  Bat_Sim_IP = 'TCPIP::172.16.4.11'
10 Multimeter_IP = 'TCPIP::172.16.4.17'
11
12 try:
13   ###################################
14   # Configuration of the device connection
15   Bat_Tester = device_connection(Bat_Sim_IP)
16   Multimeter = device_connection(Multimeter_IP)
17
18   # Start Battery Test mode
```

```
19  Bat_Tester.write(':ENTR:FUNC TEST')
20  ###################################
21  # Reset and clearing of all data for Battery Tester
22  Bat_Tester.write('*CLS')
23  Bat_Tester.write('*RST')
24  Bat_Tester.write(':SYST:ERR:CLE')
25  Bat_Tester.write(':BATT:DATA:CLE') # Clear data buffer
26  ###################################
27  # Testing configurations
28  thermistor_type = multmeter_temperature_configuration(Multimeter
        )
29
30  Bat_Tester.write(':BATT:OUTP OFF')
31
32  # Selection of operation (charge or discharge)
33  operation = input("Operation (charge or discharge): ")
34  while operation != "charge" and operation != "discharge":
35    print("Operation not recognized. Please repeat:\n")
36    operation = input("Operation (charge or discharge): ")
37
38  # Characterization of the process selected in the line above
39  voltage = input("Target Voltage (V): ")
40  capacity = input("Battery Capacity (Ah): ")
41
42  if operation == "charge":
43    charging_current = input("Charging Current (A): ")
44    battery_charge(Bat_Tester, voltage, charging_current)
45  elif operation == "discharge":
46    battery_discharge(Bat_Tester, voltage)
47
48  ###################################
49
50  # Naming of the storage file
51  filename = input("Filename: ") + '.csv'
52  filename_temp = input("Temperature filename: ") + '.csv'
53
54  # Creation and opening of the files where the samples will be
        stored
55  file_connector = open(filename, 'w')
56  writer = csv.writer(file_connector)
57  writer.writerow(['Capacity: '+ capacity + ' Ah'])
58  if operation == "charge":
59    writer.writerow(['Charging at '+ charging_current + 'A'])
60  if operation == "discharge":
61    writer.writerow(["Discharging at 1.25A"])
62
63  writer.writerow(['Voltage (V)', 'Current (A)', 'Capacity (Ah)',
        'Timestamp (s)'])
64
```

```
65  file_temp_connector = open(filename_temp, 'w')
66  writer_temp = csv.writer(file_temp_connector)
67  writer_temp.writerow(['Temperature (C)'])
68  writer_temp.writerow(["Type of Resistive device: " +
        thermistor_type])
69
70  # Start measurement process
71  Multimeter.write('DISP:TEXT "TEMP MEASURE" ')
72  Bat_Tester.write(':BATT:OUTP ON')
73  print("Output State: ", Bat_Tester.query(':BATT:OUTP?'))
74  starting_time = time.time()
75
76  cnt = 0
77  acq_error = 0
78  buff = 0
79  while 1:
80
81    if buff >= 2490: #Close to the size of the device buffer. To
          prevent any overflows
82      Bat_Tester.write(':BATT:TRAC:CLE; *OPC')
83      buff = 0
84
85    Bat_Tester.write('*OPC')
86    device_status = Bat_Tester.query(':BATT:OUTP?')
87    error_handler(Bat_Tester)
88    Bat_Tester.write('*OPC')
89
90    # Check if device finished charging/discharging
91    if int(device_status) == 0:
92      Bat_Tester.write(':BATT:OUTP OFF')
93      error_handler(Bat_Tester)
94      break
95
96    # Query the Battery tester for new values
97    data = Bat_Tester.query_ascii_values(':BATT:DATA:DATA? "VOLT,
          CURR, AH"; *WAI', converter = 's', separator = ',')
98
99    if data != ['\n']:
100     cnt = cnt + 1
101     buff = cnt
102
103     # Timestamp of the sample
104     time_elapsed = str(time.time() - starting_time)
105
106     # Query the multimeter for the temperature value
107     temp = Multimeter.query_ascii_values('READ?')
108
109     # Appending of timestamp to the battery tester sample
110     data.append(time_elapsed)
```

```
111         if len(data) == 4:
112           writer.writerow(data)
113           writer_temp.writerow(temp)
114         else:
115           acq_error = acq_error + 1
116           print("Acquisition error on sample no ", cnt)
117         if cnt % 100 == 0:
118           print("Sample no: ", cnt, " --> ", data, '|| Temperature =
                  ', temp, ' C ')
119
120     # Close connection
121     file_connector.close()
122     file_temp_connector.close()
123     Bat_Tester.write(':BATT:OUTP OFF')
124     Bat_Tester.write(':SYST:LOC')
125     Bat_Tester.close()
126     Multimeter.close()
127     print("Number of aquisition errors: ", acq_error, "\nIn
          percentage: ", round(acq_error/cnt, 3))
128 except:
129     # Print error
130     traceback.print_exc()
```

Appendix B

Project Code

```
from tabulate import tabulate
import joblib

# Importing of the models and respective data
info = joblib.load('BatEval/BatEval_Model_VFinal.sav.FhP')
battery_id = info['Bat_IDs']
wearable_data = info['Wearable_Data']
static_data = info['Static_Data']
wearable_minmax = info['Wearable_minmax']
static_minmax = info['Static_minmax']
model_wearable = info['Wearable_Model']
model_static = info['Static_Model']

manhattan_values = []
i = 0


current = float( input("Current to be supplied (A): ") )
time = float( input("Time of operation (h): ") )
temp_min = float( input("Minimum temperature ( C ): ") )
temp_max = float( input("Maximum temperature ( C ): ") )
weight = float( input("Maximum weight (g): ") )
sust = float( input("Sustainability degree[0-1]: ") )
option = input("Type of application (static/wearable): ")

```

```
26
27 if option.lower() == 'static':
28     if temp_max > static_minmax['Temp_max'][1]:
29         temp_max = static_minmax['Temp_max'][1]
30         print("Upper temperature threshold crossed. Considering
               maximum model value (65 C )")
31
32     if temp_min < static_minmax['Temp_min'][0]:
33         temp_min = static_minmax['Temp_min'][0]
34         print("Lower temperature threshold crossed. Considering
               minimum model value (-20 C )")
35
36     temp_min_norm = (temp_min - static_minmax['Temp_min'][0])/(
           static_minmax['Temp_min'][1] - static_minmax['Temp_min
           '][0])
37     temp_max_norm = (temp_max - static_minmax['Temp_max'][0])/(
           static_minmax['Temp_max'][1] - static_minmax['Temp_max
           '][0])
38     cap_norm = (current*time - static_minmax['Capacity'][0])/(
           static_minmax['Capacity'][1] - static_minmax['Capacity
           '][0])
39     weight_norm = (weight - static_minmax['Weight'][0])/(
           static_minmax['Weight'][1] - static_minmax['Weight'][0])
40
41     project_parameters = [ [temp_min_norm, temp_max_norm, cap_norm
           , weight_norm, sust] ]
42     distance, index = model_static.kneighbors( project_parameters
           )
43
44     project_parameters[0].insert(0, 0)
45     manhattan_values.append( ['Specs', '0', temp_min, temp_max,
           current*time, weight, sust] )
46     for x in index.tolist()[0]:
47         #if static_batteries[x][3]*1.0 >= weight: continue
48         if static_data[x][0]*1.0 > temp_min: continue
49         if static_data[x][1]*1.0 < temp_max: continue
50         manhattan_values.append( [ battery_id[x], distance.tolist
               ()[0][i], static_data[x][0], static_data[x][1],
               static_data[x][2], static_data[x][3], static_data[x
               ][4]] )
51         i = i + 1
52
53
54 if option.lower() == 'wearable':
55     if temp_max > wearable_minmax['Temp_max'][1]:
56         temp_max = wearable_minmax['Temp_max'][1]
57         print("Upper temperature threshold crossed. Considering
               maximum model value (65 C )")
58
```

```
59      if temp_min < wearable_minmax['Temp_min'][0]:
60          temp_min = wearable_minmax['Temp_min'][0]
61          print("Lower temperature threshold crossed. Considering
                minimum model value (-20 C )")
62
63      temp_min_norm = (temp_min - wearable_minmax['Temp_min'][0])/(
            wearable_minmax['Temp_min'][1] - wearable_minmax['Temp_min
            '][0])
64      temp_max_norm = (temp_max - wearable_minmax['Temp_max'][0])/(
            wearable_minmax['Temp_max'][1] - wearable_minmax['Temp_max
            '][0])
65      cap_norm = (current*time - wearable_minmax['Capacity'][0])/(
            wearable_minmax['Capacity'][1] - wearable_minmax['Capacity
            '][0])
66      weight_norm = (weight - wearable_minmax['Weight'][0])/(
            wearable_minmax['Weight'][1] - wearable_minmax['Weight
            '][0])
67
68      project_parameters = [ [temp_min_norm, temp_max_norm, cap_norm
            , weight_norm, sust] ]
69      distance, index = model_wearable.kneighbors(
            project_parameters )
70
71      project_parameters[0].insert(0, 0)
72      manhattan_values.append( ['Specs', '0', temp_min, temp_max,
            current*time, weight, sust] )
73      for x in index.tolist()[0]:
74          #if wearable_batteries[x][3]*1.0 >= weight: continue
75          if wearable_data[x][0]*1.0 > temp_min: continue
76          if wearable_data[x][1]*1.0 < temp_max: continue
77          manhattan_values.append( [ battery_id[x], distance.tolist
                ()[0][i], wearable_data[x][0], wearable_data[x][1],
                wearable_data[x][2], wearable_data[x][3], wearable_data
                [x][4]] )
78          i = i + 1
79
80  print('\n')
81  print('\n
        ----------------------------------------------------------------------------------------
        n')
82  print(tabulate(manhattan_values, headers=["Identification", "
        Distance", "Tmin ( C )", "Tmax ( C )", "Capacity (Ah)", "Weight
         (g)", "Sustainability"], tablefmt="fancy_grid", numalign="left
        "))
```

Appendix C

Mouse Arquitecture

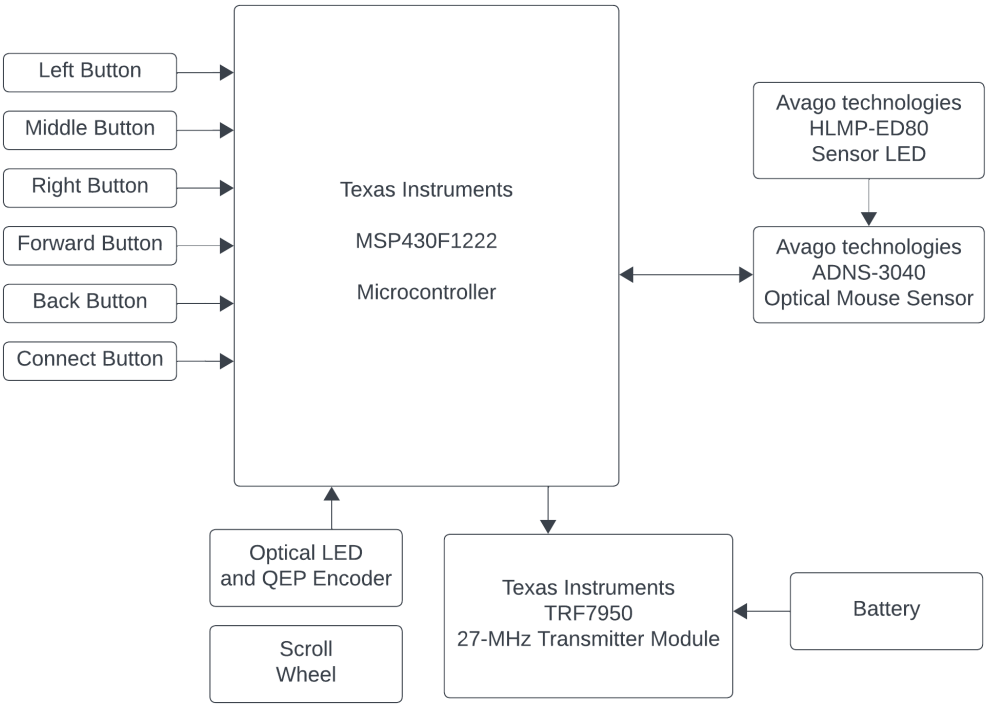

Figure C.1: Mouse Architecture (based on [83])